# Stratospheric Sulfate Aerosols impacts on West African monsoon precipitation using GeoMIP Models

Authors: Frédéric Bonou[1,2], Casimir Y. Da-Allada[1,3], Ezinvi, Baloitcha[1], Eric Alamou[1,3], Eliézer Iboukoun Biao[3], Josué E. Zandagba[1,3], Ezéchiel Obada[3], Yves Pkomalegni, Irvine Peter[4], Olivier Boucher[5] Tilmes, S[6],

[1]*International Chair in Mathematical Physics and Applications (ICMPA - UNESCO CHAIR), University of Abomey-Calavi, Benin*

[2] *Laboratory of Physics and Applications (LHA), Natitingou, National University of Sciences, Technology, Engineering and Mathematics of Abomey (UNSTIM), Benin*

[3]*Laboratory of Geosciences, Environment and Applications, National University of Sciences, Technology, Engineering and Mathematics, Benin*

[4]*Harvard John A. Paulson School of Engineering and Applied Sciences, USA*

[5]*Institut Pierre-Simon Laplace, Sorbonne Université/CNRS, Paris, France*

[6]*National Center for Atmospheric Research, Boulder, Colorado, USA*

*Corresponding Author, Frederic BONOU, ICMPA/UNSTIM, BP1076*

*Email: fredericbonou@yahoo.fr ,*

**Key Points:**

• We determine the changes of West African Summer Monsoon precipitation using stratospheric aerosol geoengineering injections climate models

• Increase of precipitation is observed under global warming while its decrease is obtained with stratospheric aerosol geoengineering models

• These changes of West African Summer Monsoon precipitation are mainly driven by the dynamic processes

**Abstract**

Stratospheric Aerosol Geoengineering (SAG) is proposed to offset global warming; the use of this approach can impact the hydrological cycle. We use simulations from Coupled Model Intercomparison Project (CMIP5) and Geoengineering Model Intercomparison Project (G3 simulation) to analyze the impacts of SAG on precipitation (P) and to determine its responsible causes in West Africa and Sahel region. CMIP5 Historical data are firstly validated, the results obtained are consistent with those of observations data (CMAP and GPCP). Under the Representative Concentration Pathway (RCP) scenario RCP4.5, a slight increase is found in West Africa Region (WAR) relative to present-day climate. The dynamic processes especially the monsoon shifts are responsible for this change of precipitation. Under RCP4.5, during the monsoon period, reductions in P are 0.86%, 0.80% related to the present-day climate in the Northern Sahel (NSA), Southern Sahel (SSA) respectively while P is increased by 1.04% in WAR. Under SAG, 3.71% of P change (decrease) was associated with a -3.51 value of efficacy in the West African Region (AR). Under G3, a significant decrease of P is found in the West

African region. This decrease in monsoon precipitation is mainly explained by changes in dynamics, which leads to weakened monsoon circulation and a shift in the distribution of monsoon precipitation. This result suggests that SAG deployment to balancing all warming can be harmful to rainfall in WAR if the amount of $SO_2$ to be injected in this tropical area is not taken into consideration.

**Plain Language Summary:**

Stratospheric aerosol geoengineering deployment has been proposed to reduce temperature increase in the context of global warming but its impacts on the hydrological cycle and its mains causes need to be strengthened on the regional scale. While the exact effects of Stratospheric aerosol geoengineering on the water cycle are uncertain, various studies suggest that there could be harmful, its consequences can cause considerable changes in regional rainfall. Climate simulations (Coupled Model Intercomparison Project: CMIP5 and Geoengineering Model Intercomparison Project GeoMIP) are used in this work to quantify their impacts on the monsoon rainfall in West Africa. We determine the changes in precipitation and its responsible mechanisms for these changes in West Africa during summer using Stratospheric Aerosol Geoengineering. Under global warming, while a slight decrease in rainfall is observed in the Sahel region. Under Stratospheric Aerosol Geoengineering, a significant decrease in rainfall is obtained over the West Africa region and the Sahel region. The main processes responsible for the changes of P under SAG are determined based on the decomposition approach, results show that changes in precipitation are largely related to changes in the dynamic processes (monsoon circulation).

**Keywords**: West Africa, monsoon precipitation, climate change, geoengineering, GeoMIP, G3, RCP4.5,

## 1. Introduction:

Climate Geoengineering is a set of some methodologies, known according to the literature as a potential way to reduce the most dangerous changes to Earth's climate as a result of large greenhouse gas increases (Launder, Brian & Thompson, J. Michael T, 2010).

Stratospheric sulfate Aerosols Geoengineering (SAG) is one of the geoengineering methods (Lenton & Vaughan, 2009) that lead to the reduction of global warming Robock et al. (2009) proved that this method could be relatively low cost, especially in comparison with the cost of mitigation, potentially making this idea attractive to policymakers and stakeholders. The reduction of incoming shortwave radiation is also called Solar Radiation Management (SRM). However, Robock et al. (2009), Tilmes et al.(2013), Kravitz et al 2013 empathized that stratospheric geoengineering with sulfate aerosols could have casual and consequences of possible impacts on the hydrological cycle, then the region of Monsoon precipitation could be impacted.. Most of the previous studies have been interested in the determination of geoengineering impacts on precipitation on the global scale (Kravitz et al., 2013; Tilmes, et al., 2013, Govindasamy and Caldeira 2000 ) have reported the reduction of the hydrological cycle with SAG applications. Although certain research works have been done, few of these works have focused on the mechanism responsible for changes in monsoon precipitation under SRM. Therefore, there is still a need to implement the analysis of the hydrological cycle on a regional scale under SRM and to determine the mechanisms responsible for changes in P using the existing climate models.

The West African monsoon (WAM) is a system of Earth's climate, that involves interconnections between the atmosphere, the biosphere, and the hydrosphere over many time scales during the boreal summer (e.g. Nicholson and Grist 2003; Redelsperger et al. 2006). It is part of the global monsoon system, which regulates atmospheric humidity and heat budgets in low latitudes. It is the major source of water for agriculture in West Africa (Froidurot & Diedhiou, 2017), it is the principal determinant of agricultural production in densely populated areas where the economy is dependent on subsistence farming. The WAM precipitation is characterized by moisture fluxes derivation from different sources comprising the soil moisture and the atmospheric moisture flux convergence (Gong & Eltahir, 1996; Lélé et al., 2015; Mera et al., 2014). Some previous works investigated the atmospheric moisture over the WAM, (Pomposi et al. (2015) observed that changes in moisture flux convergence, as well as the circulation process within the higher precipitation region and along the monsoon border, are associated with the precipitations changes within the Intertropical Convergence Zone (ITCZ). (Xue & Shukla .(1993) demonstrated that the role of continental surfaces is linked by the soil moisture and precipitation in the WAM region. In the West African monsoon (WAM) zone, the role of continental surfaces is fully verified due to the close relationship associated with soil moisture and precipitation (Xue & Shukla, 1993). Interesting descriptions of the WAM hydrology and dynamics have been described in many works (J. L. Redelsperger et al., 2001).

The West African (WA) Monsoon precipitation variability poses a constraint to the water resources, vegetation, and food security and its long-term state over periods of few years

to several decades has been investigated thoroughly (Abiodun et al., 2008; Janicot, 1992; Lamb, 1982; Nicholson, 2013; Okoro et al., 2018; Sanogo et al., 2015). The WAM precipitation results from the moisture fluxes originating from many sources during the summer season. More than 80% of the annual rainfall occurs during June–September when the intertropical front is northward position, but the total precipitation has annual variations (Le Barbé et al., 2002). WAM region frequently suffers from droughts, which cause water deficiencies and disrupt the agriculture sector; this is the only sector that provides both food and income for the majority of rural households. The impact of these droughts and the controversy concerning their causes has prompted climatologists to offer a variety of hypotheses including changes in the ITCZ latitude position, tropical Atlantic sea surface temperature anomalies, energy balance changes. The WAM contributes to the majority of summer precipitation in the Sahel(Dong & Sutton, 2015). The WAM's transition to its strong phase is related to wind forcing, evaporation, Sea Surface Temperature (SST) positive feedback (S.P. Xie, 1999): warming in SST in the northern part of Atlantic relative to that of southern drives stronger-westerly winds forcing and intensify the WAM, which reduces surface evaporation north of the equator and enhances it in the South, amplifying the interhemispheric SST gradient.

Increased WAM, induced by anthropogenic greenhouse gas and aerosol forcing, may have led to a significant increase in Sahel precipitation since the 1980s (Dong & Sutton, 2015). Under RCP 8.5, approximately 80% of CMIP5 models agree on a modest drying rate of around 20% over the westernmost Sahel (15°W–5°W), whereas approximately 75% of models agree on an increase in precipitation between 0°E and 30°E over the Sahel, with a wide amplitude distribution (Roehrig et al., 2013). The projected reinforcement of WAM is related to a robust expansion of warming over the Sahel by around 10%-50% over the global mean (Roehrig et al., 2013). Several works basing on SAG emphasized that the offset of global warming may cause a reduction of global precipitation (Bala et al., 2008; Govindasamy & Caldeira, 2000; A. C. Jones et al., 2018; Robock et al., 2008; Tjiputra et al., 2016; Xu et al., 2020, Odunlami et al., 2020 ). Some of these works pointed out the weakening of precipitation over the monsoon land regions such as the West African Summer Monsoon region under SAG (e.g., Cheng et al., 2019; Dagon & Schrag, 2016, 2017; Haywood et al., 2013; Niemeier et al., 2013; Robock et al., 2008; Tilmes et al., 2013). Recent work by Pinto et al.(2020) argued that the application of SAG will impact temperature and rainfall means and extremes over sub-Saharan Africa using simulations GLENS. They found agree that the use of SAG leads to a reduction in temperature means and extremes precipitations, it has been shown that the use of SAG in the northern hemisphere only could affect the hydrological cycle in the Sahel, while the SAG injection in only the Southern Hemisphere may increase significantly the Sahel vegetation productivity (Haywood et al., 2013). These authors showed that the injection of SAG in only one hemisphere may impact the position of the Inter tropical Convergence Zone (ITCZ). Some Recent studies demonstrated that the control of temperature variation through multiple aerosol injections at several latitudes, as in the Geoengineering Large Ensembles (GLENS) simulations (Tilmes et

al., 2018), may lead to reduce shifts in the latitude of the ITCZ and related rainfall (Cheng et al., 2019; Kravitz et al., 2017, 2019; MacMartin et al., 2019; Tilmes et al., 2018; Xu et al., 2020) Interpreting variations in global mean precipitation, Kravitz et al.(2013) described the changes in the surface and atmospheric energy budgets using GeoMIP simulations (Kravitz et al., 2011) and they reported that changes in precipitation could be attributed to a decrease in the mean flux of evaporative moisture and increased moisture convergence, particularly over land regions. Furthermore, using GeoMIP simulations, Kravitz et al.(2013) and Tilmes and et al.(2013) reported the large decline in land evaporation in most regions associated with the global decline in precipitation, this is not the case in the rainfall regions of the summer monsoon, such as the West Africa region, whereas summer monsoon rainfall is influenced by both regional and large scale processes. Consequently, the mechanisms responsible for changes in West African Monsoon Summer precipitation need to be implemented. Changes in tropical precipitation can be demonstrated through the decomposition into the contributions of thermodynamic and dynamic processes (e.g., Weller et al., 2019), and the decomposition methodology of (Chadwick et al., 2013, 2016) can be used to identify the related contribution of these two terms (Da-Allada et al., 2020; Chadwick et al., 2016; Kent et al., 2015; Lazenby et al., 2018; Monerie et al., 2019). Using this method, changes in tropical precipitation, under climate change, have been largely associated with changes in the dynamic component indicating changes in the position (Chadwick et al., 2016; Kent et al., 2015). Due to the great importance of West African Summer Monsoon (WASM) precipitation on agriculture productivity, the magnitudes and patterns of WAM system responses to geoengineering need to be investigated regionally, and climate modeling should be a helpful way in this analysis. The use of climate geoengineering is expected to balance the warming resulting from increasing concentrations of greenhouse gases with a corresponding decrease in solar absorption (Crutzen, 2006) associated with precipitation reduction. Geoengineering atmosphere models basing on sulfate aerosols also show changes in stratospheric dynamics and chemistry caused by SRM (Heckendorn et al., 2009; Tilmes et al., 2009). Recently, Da-Allada et al. (2020) found that the dynamic process is the main mechanism responsible for the change of WASM using GLENS simulations. By subdividing the West African region into three sub-regions, they found that the deployment of SAG in North of Sahel (NSA) and South of Sahel (SSA) could be effective while their application in West Africa Region (WAR) can be over effective.

In the current study, the changes under SRM on West African Monsoon precipitation have been determined using GeoMIP (G3/G4) and Coupled Model Intercomparison Project CMIP5 (Historical, RCP4.5) simulations after validation with CMAP and GPCP observations. These impacts of SRM are determined in the context of global warming and climate geo-engineering with their main causes to explain the changes obtained. The rest of the manuscript is organized as follows, Methods and data , the section in which present the set of data and methods used in this study. Results describe the validation of historical simulation in regards to CMAP and GPCP observations. The impacts of SRM on WAM precipitation are presented in this same section under different simulations. The potential mechanisms explaining the changes in

monsoon precipitation have been determined basing IPSL-CM5A-LR due to availability of specific humidity with higher vertical resolution. The Discussion section is dedicated to the results discussion. Finally, the conclusion presents a summary of the results obtained in this paper.

## 2. Methods and data

Ten CMIP5 era climate models with 2 experiments (Historical and RCP4.5 simulations) are analyzed in this paper; these models are listed in Table 1. These Historical CMIP5 models are extracted from the global data for West Africa during the monsoon period (Fig .1). Two observations data of precipitation data (GPCP and CMAP) have been used for the comparison with historical data. This set of models have been chosen due to the availability of GeoMIP (G3/G4) simulations associated with CMIP5 simulations. These distributions of Historical precipitation in West Africa staring from 1986 to 2005 (20 years). The analysis focuses on the seasonal average of West African Monsoon precipitation mainly during boreal summer, the monsoonal season starting from July to October (JASO) according to (Da-Allada et al., 2020; Gaetani et al., 2017) in this area. For each model, daily or monthly data from (historical experiments of CMIP5 models) are analyzed jointly with RCP4.5 (CMIP5). The CMIP5 models have different simulations; their Historical simulations are the simulations of the recent past (Sheffield et al., 2013). The CMIP5 Historical simulations are the simulation in which all forcing have been applied to the models, including anthropogenic greenhouse gas concentrations. The historical simulation began from multicentury preindustrial control runs and configured with the observed atmospheric composition evolution (anthropogenic and natural sources) The RCP4.5 is the Representative Concentration Pathway (RCP 4.5) with a scenario that provides stabilization to radiation forcing at 4.5 $W.m^{-2}$ in with future projection starting from 2006 to 2100 without ever exceeding that value. This simulation incorporates historical emissions and land cover information. We used in this study the GeoMIP climate era models with two experiments (G3/G4) simulations. G3 is a combination with RCP4.5 forcing, starting in 2020, gradual ramp-up the amount of $SO_2$ or sulfate aerosol injected, to keep global average temperature nearly constant (Kravitz et al., 2011). G4 is a combination with RCP4.5. Starting from 2020, it requires continuous injection of $SO_2$ through the lower stratosphere to the equator at a rate of 5 Tg $SO_2$ per year (Kravitz et al., 2011, Bürger et al., 2015, Clarke et al., 2021). We used monthly RCP4.5 and G3 and G4 simulations, monthly historical P simulations of CMIP5 have been compared with the observations for model validation over 1986 and 2005.

The changes in rainfall have been calculated through the difference between all the existing ensemble members of RCP4.5 over 2050–2069 and the baseline (present-day climate: 2010–2029) under global warming. Under SAG, changes of P have been quantified through the difference between the only ensemble member of G3 (2050-2069) and baseline (Table 1). We select this future period (2050-2069) as the distribution of $SO_2$ injection rates converges around 2050 (MacMartin et al., 2019). The baseline period is 20 years (2010–2029), which is

considered as the period more suitable for present–day climate. The statistical significance of the rainfall changes is determined using a two-tailed Student's t-test and the standard error is used to provide an estimate of the error in the rainfall changes

The Earth System Models (Dufresne et al., 2013), has been generally developed in different institutions. IPSL-CMA5-LR, is one of the atmospheric models based on LMDZ5 (Hourdin et al., 2013), with different horizontal resolution and vertical levels. The ocean model coupled with that of atmospheric is NEMOv3.2 (Madec, 2016), in ORCA2 configuration. The performances of the oceanic component in the coupled configuration are presented in Mignot et al. (2013) for the case of IPSL-CMA5-LR. More information on this model can be found in the special issue in Climate Dynamics (http://link.springer.com/journal/382/40/9/) for a collection of studies describing various aspects and components of the model as well as its performance. The high resolution IPSL-CMA-LR for the specific humidity, the version with CMIP table (CFday) of geoengineering model has been used to determine the potential mechanisms to the impact of SRM on the West African Monsoon Precipitation. NCAR Climate Variability Diagnostics Package (Phillips et al., 2014), or diagnostics such as the cloud regime metric (Williams and Webb, 2009) developed by the Cloud Feedback MIP (CFMIP) community.

The availability of high vertical resolution of specific humidity (Hus) at different levels of pressure in IPSL–CM5A-LR is an advantage for the determination of mechanisms responsible for P changes using decomposition methods. The main variables extracted from each simulation in this work are monthly precipitation (P). Additional parameters such as daily wind velocity (V), specific humidity (q) has been used due to the high vertical resolution of CF convention simulation of IPSL-CM5A-LR. For the validation of Historical simulation, Monthly precipitation data used in this study were obtained from the Climate Prediction Center (CPC) Merged Analysis of Precipitation (CMAP) dataset (P. Xie & Arkin, 1997) from 1979 to 2018, Global Precipitation Climatology Project (GPCP) data estimates on a 2.5 × 2.5 degree latitude/longitude (Huffman et al., 1997) were used in this study. Precipitation change (ΔP) has been decomposed into dynamical (ΔPdyn), thermodynamical (ΔPtherm) and non-linear cross components (ΔPcross) according to Chadwick et al.(2016) to access the causes of precipitation changes in WA under SRM. In reality, this method assumes that the precipitation is dominated by convection in tropical region (Chadwick et al., 2016; Monerie et al., 2019). The precipitation, P, is considered as P = M*q, where M* is defined as a proxy for convective mass flux from the boundary layer to the free troposphere (Held & Soden, 2006; Kent et al., 2015; Lazenby et al., 2018), M* = P/q, and q is near surface specific humidity, then, the change in rainfall , then, ΔP c is decomposed as :

$$\Delta P = M^*\Delta q + q\Delta M^* + \Delta q\Delta M^* \quad \text{(Eq .1)}$$

$$= \Delta P_{therm} + \Delta P_{dyn} + \Delta P_{cross}$$

where erm + ΔPdyn + ΔPcross thermodynamic change due to the specific humidity changes (q), ΔPdyn represents the dynamic change from circulation changes (M*), and ΔPcross is the term due to the changes in both specific humidity and circulation. Further decomposition of ΔPdyn allows us to document changes due to shifts in the pattern of circulation (ΔPshift) or the mean

tropical circulation (ΔPweak), as

$$\Delta P_{dyn} = \Delta P_{weak} + \Delta P_{shift} \quad \text{(Eq 2)}$$

$$\Delta P_{weak} = q\Delta M^*_{weak} \quad \text{(Eq 3)}$$

$$\Delta P_{shift} = q\Delta M^*_{shift} \quad \text{(Eq 4)}$$

$$\Delta M^*_{weak} = -\alpha M^* \quad \text{(Eq 5)}$$

where $\alpha$ = (tropical mean $\Delta M^*$)/tropical mean $M^*$ is the change in the weak of the mean tropical circulation. Note that although $\Delta M^*$ is a scalar, $\Delta P_{weak}$ is provided for each grid point by multiplying by the reference moisture field. $\Delta M^*_{shift}$ is calculated by the difference $\Delta M^*$ and $\Delta M^*_{weak}$.

Table 1: List of Models used in this work

| Models | G3(members) | G4 (members) | Historical (Members) | Rcp45(members) | Reference |
|---|---|---|---|---|---|
| BNU-ESM | 1 | 1 | 1 | 1 | (Verten-stein et al., 2010) |
| CanESM2 | Not available | 3 | 4 | 10 | (Chylek et al., 2011) |
| CSIRO-MK3L-1-2 | Not available | 3 | 4 | 3 | (Parth et al., 2016) |
| GISS-E2-R | 3 | 3 | 9 | 3 | Schimidt et al., 2014 |
| HadGEM2-ES | 3 | 3 | 4 | 4 | (Collins et al., 2011) |
| IPSL-CMA-LR | 1 | Not available | 6 | 5 | Dufresne et al.(2013 |
| MIROC-ESM | 1 | 1 | 3 | 3 | (Watanabe et al., 2011) |
| MIROC-ESM-CHEM | Not available | 9 | 1 | 9 | (Watanabe et al., 2011) |
| MPI-ESM-LR | 3 | Not available | 3 | 3 | Mauritsen et al., 2019 |
| NorESM1-M | 2 | 1 | 3 | 1 | Bentsen et al., 2013 |
| GEOSCCM | | 3 | Not available | 3 | Douglass et al., 2004 |
| CNRM-ESM1 | | 4 | 1 | 4 | Séférian et al., 2016 |

-G3, G4 and RCP4.5 simulations: 2050-206
- Baseline simulations (RCP4.5): 2010-2029
- CMIP5 historical simulations: 1986-2005:

## 1. Results and Discussion

### 3.1 validation of historical simulation

Historical simulations basing on Precipitation from CMIP5 models have been compared with GPCP and CMAP observations over the same period (Fig. 1. and 2). Most of the CMIP5 simulations used in this work are relatively in the agreement with the observations (CMAP,

GPCP), the maxima of precipitation in the West African region are mostly represented approximately over the band located between 10°S to 10°N during African Monsoon period, although some differences in the position of the maxima of P appears in the extension of high precipitation southward from one simulation to another (Fig. 1). All historical simulations present a slight underestimation from one subregion to another in West Africa region (Fig. 1). The CSIRO simulation exhibits a higher underestimation of rainfall while CNR-ESM1 presents an overestimation of rainfall compared with GPCP and CMAP (Fig 2). However, the zone of the P maxima zone is well represented. Mostly, all models agree with the maxima of P distribution, from the ocean to the countries with an intensification of P during the monsoonal period (with the values reaching ~10 mm.d$^{-1}$)

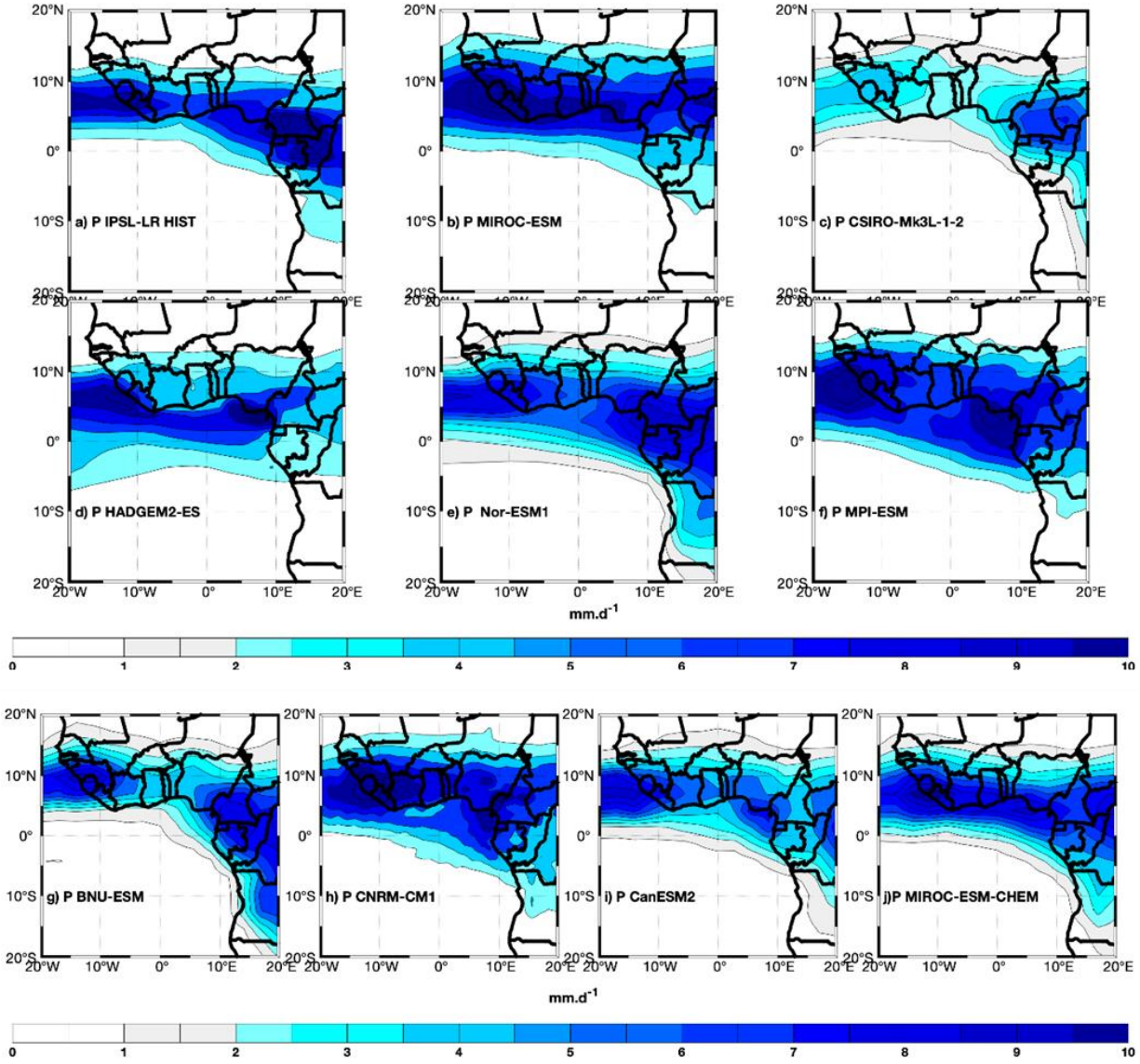


**Figure 1**: Spatial distributions of monthly precipitation (mm. day -1.) averaged over 1986-2005 between July and October in West Africa from **a)** to **j**) from CMIP5 models

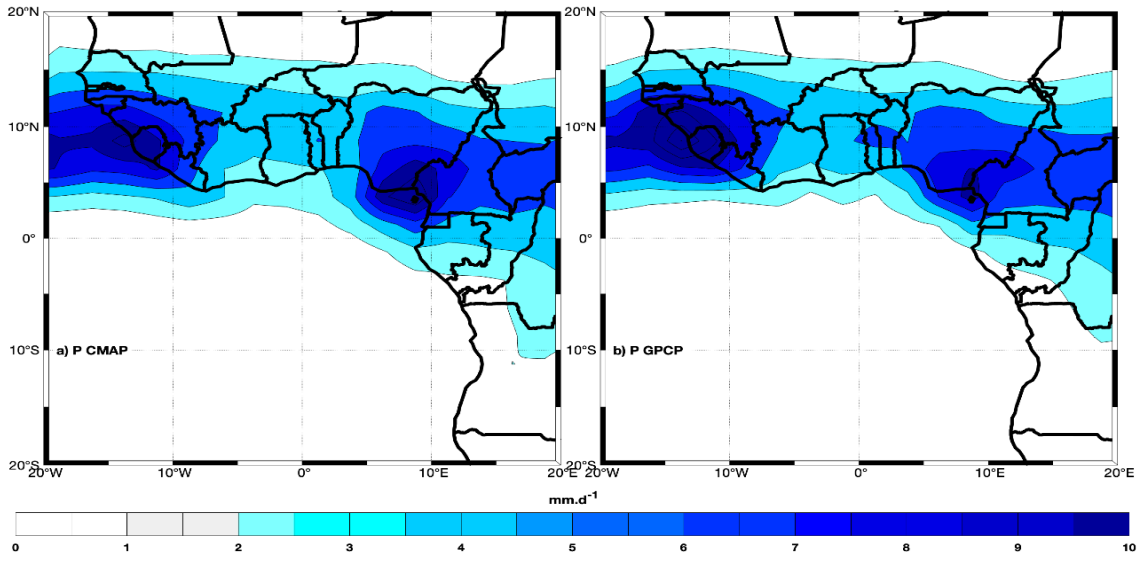


**Figure 2:** Spatial distributions of monthly precipitation (mm. day -1.) averaged over 1986-2005 between July and October in West Africa from **a** to i) from CMAP and GPCP data

The performances of each Historical CMIP5 precipitation in West Africa are statistically summarized basing on Taylor diagram (Fig. 3) to identify the models which are close with observation data. This diagram provides a concise statistical evaluation of the degree of pattern correspondence between the models and observations regarding their Pearson's correlation (Cor), root-mean-square error (RMSE), and the ratio of their variances (STD). All simulations reproduce the monsoonal precipitation referenced CMAP precipitations, but also to GPCP observations. in West Africa (Fig. 3).

**Figure 3:** Taylor diagrams showing monthly precipitation averaged over 1986-2005 between July and October in West Africa. The red dot denotes the CMAP observations data.

The analysis of precipitation biases is described through the estimation of the difference between each model and the CMAP observations. Negative changes (~ 5 $mm.day^{-1}$) have been observed over West Africa and Sahel region from one model to another. IPSL-CM5A-LR, MIROC-ESM-CHEM, HadGEM2-ES, MPI-ESM, Nor-ESM1, BNU-ESM, CanESM2 all show an underestimation of precipitation over the Sahel region while a modest overestimation can be observed over West Africa and coastal regions (Fig. 4). CSIRO-Mk3L-1-2 mostly shows strong underestimation compare to the observation over the West Africa and the Sahel region. The ensemble simulations of CMIP5 models show that their historical simulations are less rainy over Sahel region while strong precipitations are distributed over some coastal countries and the southern part of West Africa.

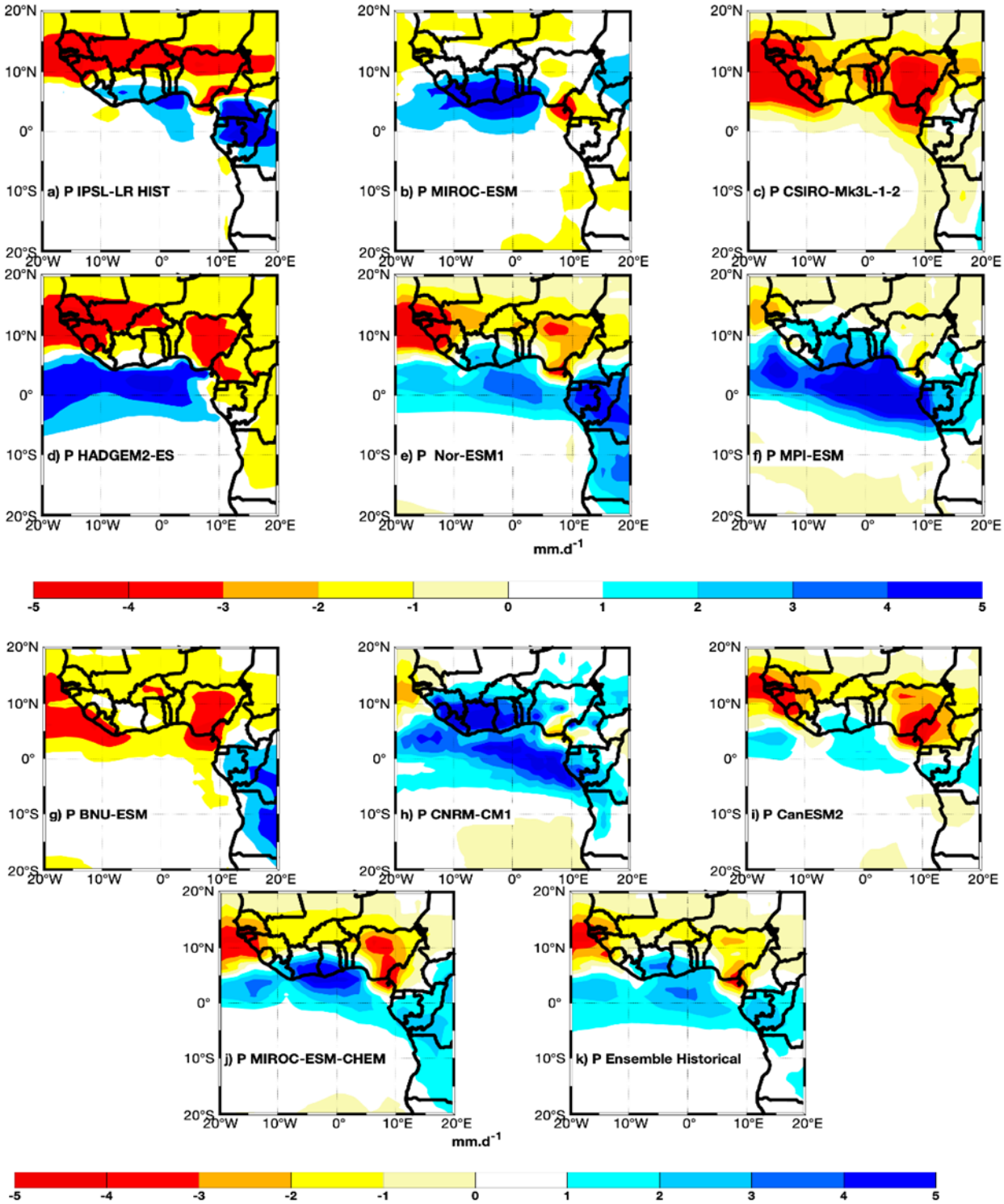


**Figure 4**: Difference of precipitation between Models and CMAP observations between July and October

### 3. 2 Impact of global warming and Stratospheric aerosol injection on monsoon P

The changes of precipitation under different G3 simulations have been estimated by calculating the difference between G3 and baseline simulations (RCP4.5, from 2010 to 2029). Most of the models present the decrease of precipitation over the West Africa region (Fig.5), and Sahel region following by GIESS-E2R simulation which presents also increase of precipitation mainly over West Africa. Due to the high influence of both previous models, the ensemble G3 simulations show a slight increase in precipitation under the present-day simulation. The Table 2 below presents the different values of the difference between each G3 simulations and the baseline simulation, the mean bias error (MBE) and their root mean square error (RMSE)

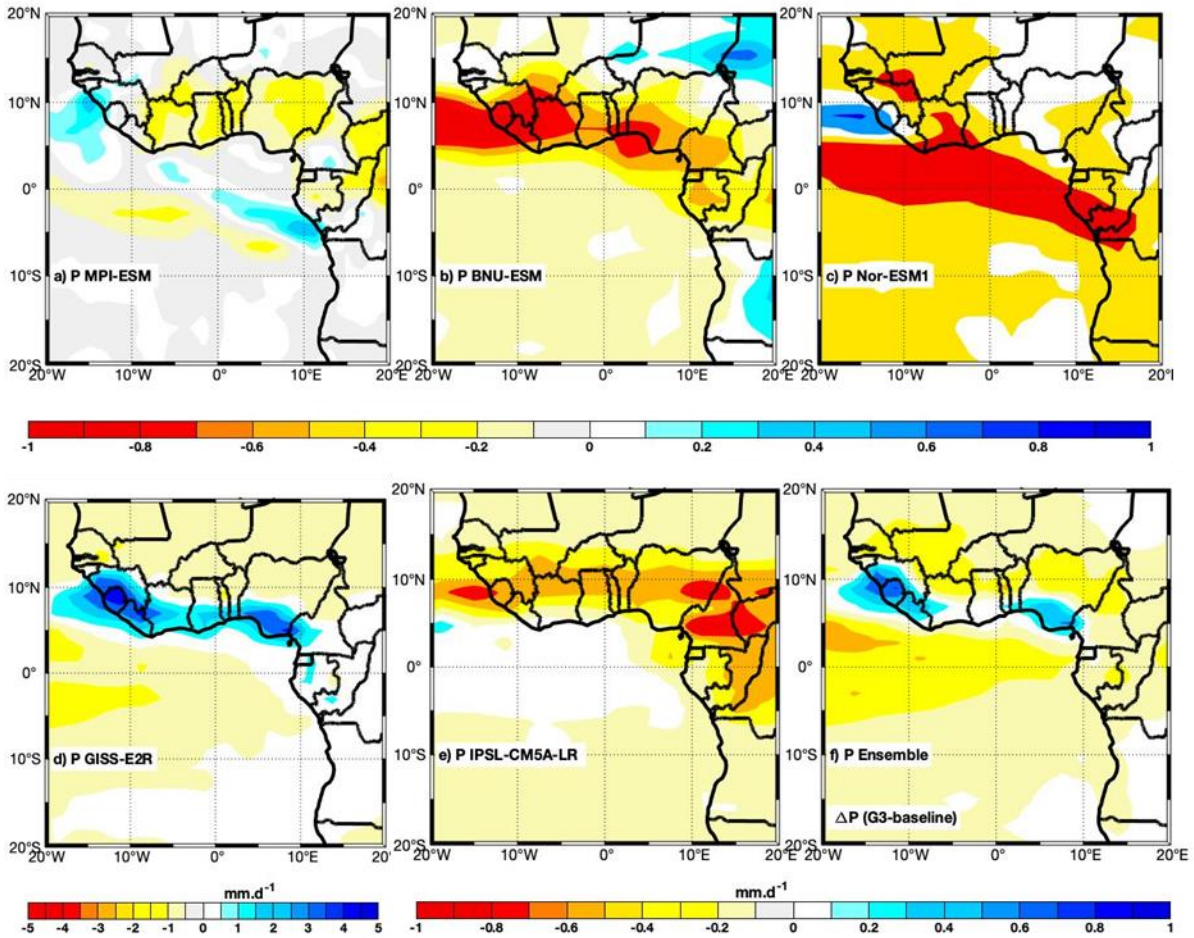


**Figure 5:** Changes of precipitation between Models and baseline(G3-baseline) simulations during the monsoon period

Table 2: Mean bias error (MBE) and root mean square error (RMSE) between G3 and baseline simulations. All MBE values are significant ( t-test, $p<0.05$)

| Model | MBE | RMSE | Percentage (%) |
|---|---|---|---|
| MPI-ESM | -0.2007 | 0.0597 | 2.4 |

| | | | |
|---|---|---|---|
| BNU-ESM | -0.2572 | 0.0323 | 6.8 |
| Nor-ESM1 | -0.6305 | 0.1324 | 8.9 |
| HadGEM2-ES | 3.3784 | 0.3784 | |
| GISS-E2R | 0.3176 | 0.0916 | 6.8 |
| IPSL-CM5A-LR | -0.0450 | 0.1145 | 0.64 |
| Ensemble | 0.4452 | 0.0559 | 7.8 |

G4 simulations are the second scenarios analyzed in this study as one of the SAG scenarios. The changes of precipitations are also estimated by retrieving its associated baseline (Fig.6). The models, BNU-ESM, CSIRO-Mk3L-1-2 and GEOSCM show relatively the decrease (~1mm.day-1) of precipitations over West Africa and Sahel regions. However. MIROC-ESM, MIROC-ESM-CHEM present the increase of P over Sahel region.This set of models affect the ensemble simulation which presents a higher increase of precipitation over West Africa and G4 simulation (Table 3). All these mean bias errors (MBE) are tested statistically significant student test ($p<0.05$) except that of GEOSCCM.

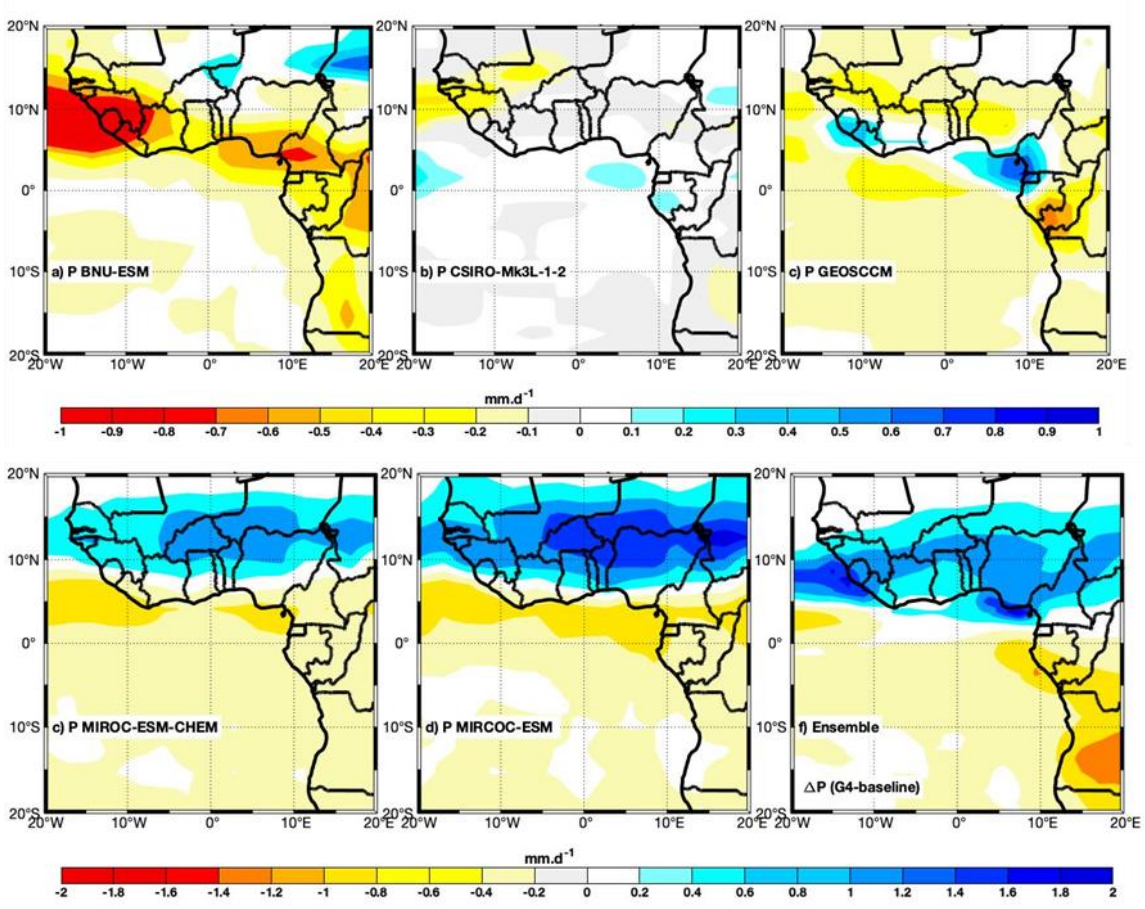


Figure 6: Changes of precipitation between Models and baseline(G4-baseline) simulations during monsoon period

Table 3: Mean bias error (MBE) and root mean square error (RMSE) between G4 and baselines simulations, all values are significant (t-test, $p<0.005$) except the MBE of GEOSCCM

| Model | MBE ($mm.day^{-1}$) | RMSE((mm.day-1) | Percentages (%) |
|---|---|---|---|
| MIRCOC-ESM | -0.5030 | 0.1033 | 6.5 |
| HadGEN2-ES | 3.4157 | 0.3452 | |
| BNU-ESM | -0.2992 | 0.0551 | 6 |
| CSIRO-Mk3L-2-2 | 0.0677 | 0.0342 | 2.6 |
| MIROC-ESM-CHEM | -0.4450 | 0.0778 | 7 |
| GEOSCCM | 0.0073 | 0.0893 | 0.01 |
| Ensemble | 0.3865 | 0.2387 | 6.4 |

### 3.2.1 Precipitations changes under global warming (RCP45-baseline)

Under global warming, the changes of precipitation have been estimated by calculating the difference between each RCP4.5 model and its baseline simulation. Different trends of precipitations changes have been observed over West Africa and the Sahel region (Fig. 7). The ensemble simulation exhibits mostly the increase of precipitation over West Africa and Sahel region. The results vary from one model to another. Negatives changes are observed over West Africa and the Sahel region with MPI-ESM, BNU-ESM, Nor-ESM1, and MIRCOC groups Models (Table 4). This trend of precipitations with these simulations is opposite to that of the rest of RCP4.5 simulations and the ensemble simulations.

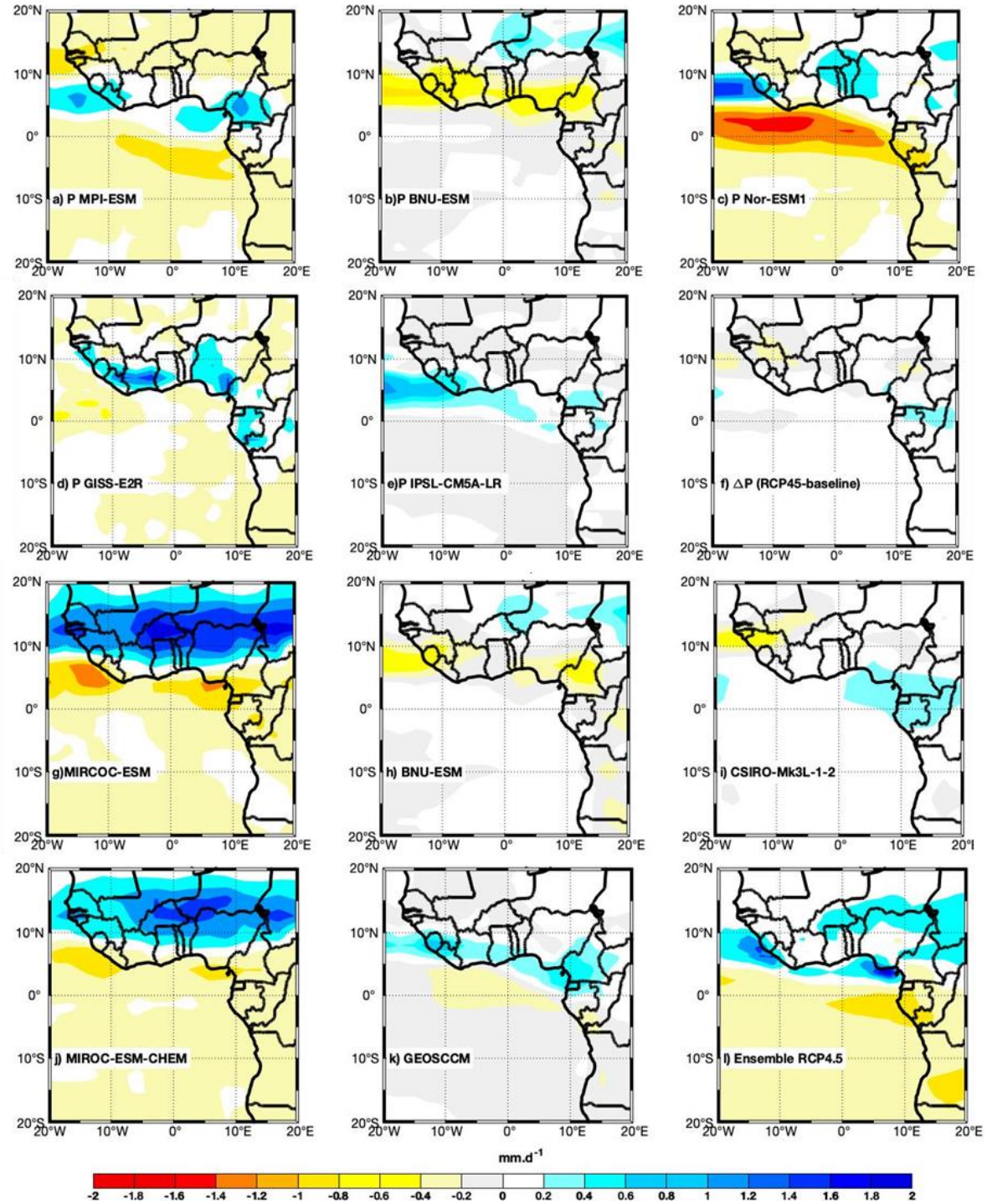


**Figure 7:** Changes of precipitation between Models and baseline (RCP4.5-baseline) simulations during the monsoon period

Table 4: Mean bias error (MBE) and root mean square error (RMSE) between RCP4.5 and baseline simulations

| Model | MBE | RMSE | Percentage of changes (%) |
|---|---|---|---|
| MPI-ESM | -0.1392 | 0.1323 | 1.6 |
| BNU-ESM | -0.0781 | 0.0518 | 2.1 |
| Nor-ESM1 | -0.4599 | 0.1228 | 6.6 |
| GISS-E2R | 0.0895 | 0.0651 | 1.9 |
| IPSL-CM5A-LR | 0.2376 | 0.1205 | 3.4 |
| MIROC-ESM | -04945 | 0.0785 | 6.4 |
| CSIRO-Mk3L-2-2 | 0.1867 | 0.1867 | 7.2 |
| MIROC-ESM-CHEM | -0.3174 | 0.663 | 5 |
| GEOSCCM | 0.0279 | 0.0001 | 0.04 |
| Ensemble | 0.4294 | 0.0534 | 10 |

The IPSL-CM5A-LR models are used in this work to analyze the mains mechanism driven precipitations changes under SAG and global warming. The reason for that choice is basing on the availability of specific humidity data at pressure levels near 950hPa in IPSL-CM5A-LR as used in (Da-Allada et.al, 2020). In this work, RCP4.5 simulations have been chosen as G3 simulations derived directly from RCP4.5. Under RCP4.5 at global warming conditions, the monsoonal precipitation change is determined by computing the difference of P between two different periods (RCP4.5: 2050–2069) relative to baseline (RCP4.5: 2010-2029) as recently done by Da-Allada et al. (2020) with GLENS simulations. An increase in summer monsoon precipitation is most observed toward the oceanic zone adjacent to the West Africa region (Fig. 8a) associated with the slight increase of P in West African region. All the West Africa countries are not affected by this P change on P, it is important to note that this increase observed is not statistically significant. However, the main processes responsible for the P changes (ΔP) under RCP4.5 is due to monsoon precipitation shifts distribution (ΔPshift), otherwise the dynamic process (Fig 8b-d) similar mechanism with the results of Da-Allada et al. (2020) who also found the dynamic process as the mains mechanism responsible of P change under RCP8.5 with GLENS simulations. The ΔPcross contribution is low toward to precipitation changes (Fig. 8c). The increase of ΔPtherm distribution is also observed from the equator toward the north part, this pattern also contributes slightly to the change of P observed under global warming (Figs. 8b and 8g). This pattern of ΔPtherm is explained by the increase of specific humidity (Fig 8a and 8b). ΔPdyn distribution shows mostly a decrease between 5°- 10°N. A slight decrease (~ -0.1 $mm.day^{-1}$) appears over the Sahel region (Both North and South region) under RCP4.5 simulation, contrary patterns have been recently found by Da-Allada et al. (2020).

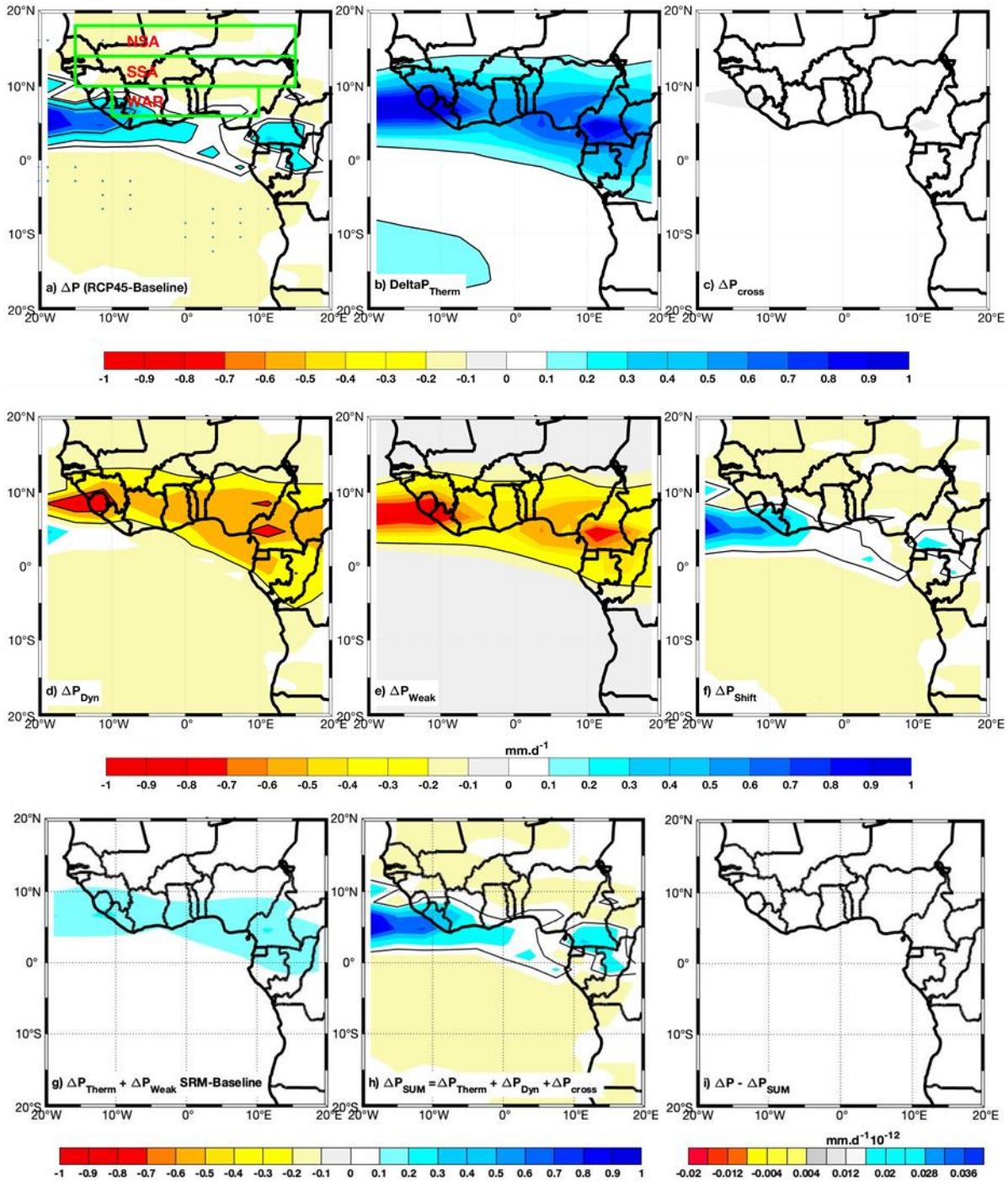


Figure 8: (a) Changes in monsoon precipitation under RCP4.5 related the baseline with its different terms, (b) thermodynamic (ΔPtherm), (c) nonlinear cross term (ΔPcross) and (d) dynamic (ΔPdyn). The dynamic component (ΔPdyn) is decomposed into (ΔPweak) and (ΔPshift). The Fig 8.g presents the sum of ΔPtherm+ ΔPweak, h) presents the sum of ΔPtherm + ΔPcross+ ΔPdyn, the difference between Fig8.a (the model precipitation change) and Fig8.h (the sum of all the components of precipitation change).

ΔPdyn term has been decomposed according to Equation 2 by dissociating this term into a term associated with the weakened low-level monsoon (ΔPweak) and a term associated with the local dynamic feedback in charge of monsoon precipitation shifts distribution (ΔPshift). The spatial distribution of ΔPweak presents the constrat pattern with ΔPtherm (Fig. 8.b and 8.e). The amplitude of ΔPtherm is dominant over that of ΔPweak, as their sum remains positive (Fig 8.g). The distribution of ΔPshift has a similar patterns trend as that of P (Figs. 8.a and 8.f). The ΔPshift has a similar pattern of distribution as the ΔP, thus ΔPshift component of ΔPdyn is responsible for the changes in ΔP. The change of precipitation under RCP4.5 based on the decomposition method is similar to the change in P (Figs 8.a and 8.h) and their difference is null (Fig. 8i), emphasizing that the decomposition method used is consistent to demonstrate changes in West African Monsoon precipitation. The similar concept has been used by Da-Allada et al. (2020) to explain the changes basing on P decomposition. In conclusion, the changes in precipitation under RCP4.5 are mainly driven by the dynamic process.

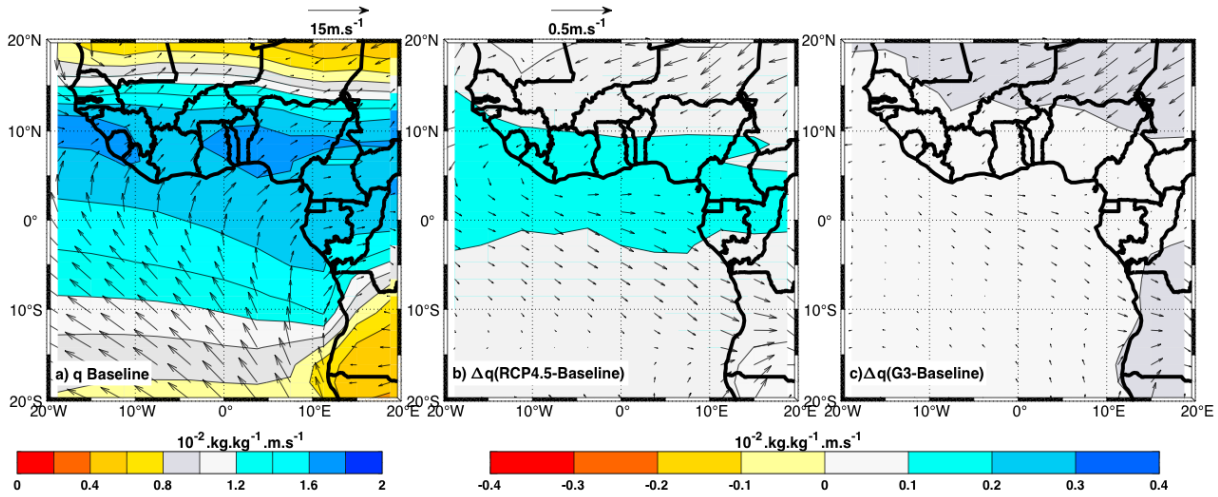


**Figure 9:** Spatial distributions of average monthly near surface specific humidity (in color) and surface wind field (vectors) at 955 hPa for the baseline simulation over 2010-2029, b) differences (relative to the baseline) in mean surface specific humidity (color) and near-surface wind (vectors) under RCP4.5, 2050-2069 at same pressure level and c) same as in b with G3 simulation)

### 3.3- Impacts of P changes and its main causes under G3

Under SAG, the spatial monthly distribution of P in G3 simulation relative to that of baseline shows the decrease in summer monsoon precipitation in West African regions (Fig.

10.a) This change of P is similar to that obtain in Da-Allada et al. (2020) who determined the decrease of P under G3 simulation of GLENS model over this region. This precipitation change is also significant in West African Countries (Fig. 10.a). As in the RCP4.5, the contribution of ΔPcross to precipitation changes is also negligible under G3 simulations (Fig. 10.c). ΔPtherm does not contribute to precipitation change under G3 due to the lower difference in the near-surface specific humidity compared with the baseline (Fig. 9.c and Fig 9.b). The contribution of dynamic terms (both weak and shift terms) explains the change in P under G3, from both components, the ΔPweak component has a similar magnitude as that of P, but it is also noted the contribution ΔPshift with a decrease (~0.2 $mm.day^{-1}$), therefore both these terms of dynamic terms can explain the decrease in precipitation (Figs. 10.a, 10.e and 10.f). Their contribution is largely associated with the low-level land-sea temperature contrast (Da-Allada et al., 2020). The change in monsoon rainfall under G3 primarily based on the decomposition approach is equal to the change in precipitation simulated (Figs. 10.a and 10.h) and the difference between these two terms is negligible (Fig. 10.i). In conclusion, under G3, change in precipitation is explained by the dynamical process, that leads to weakened monsoon circulation of the monsoon precipitation distribution and a shift in the monsoon precipitation.

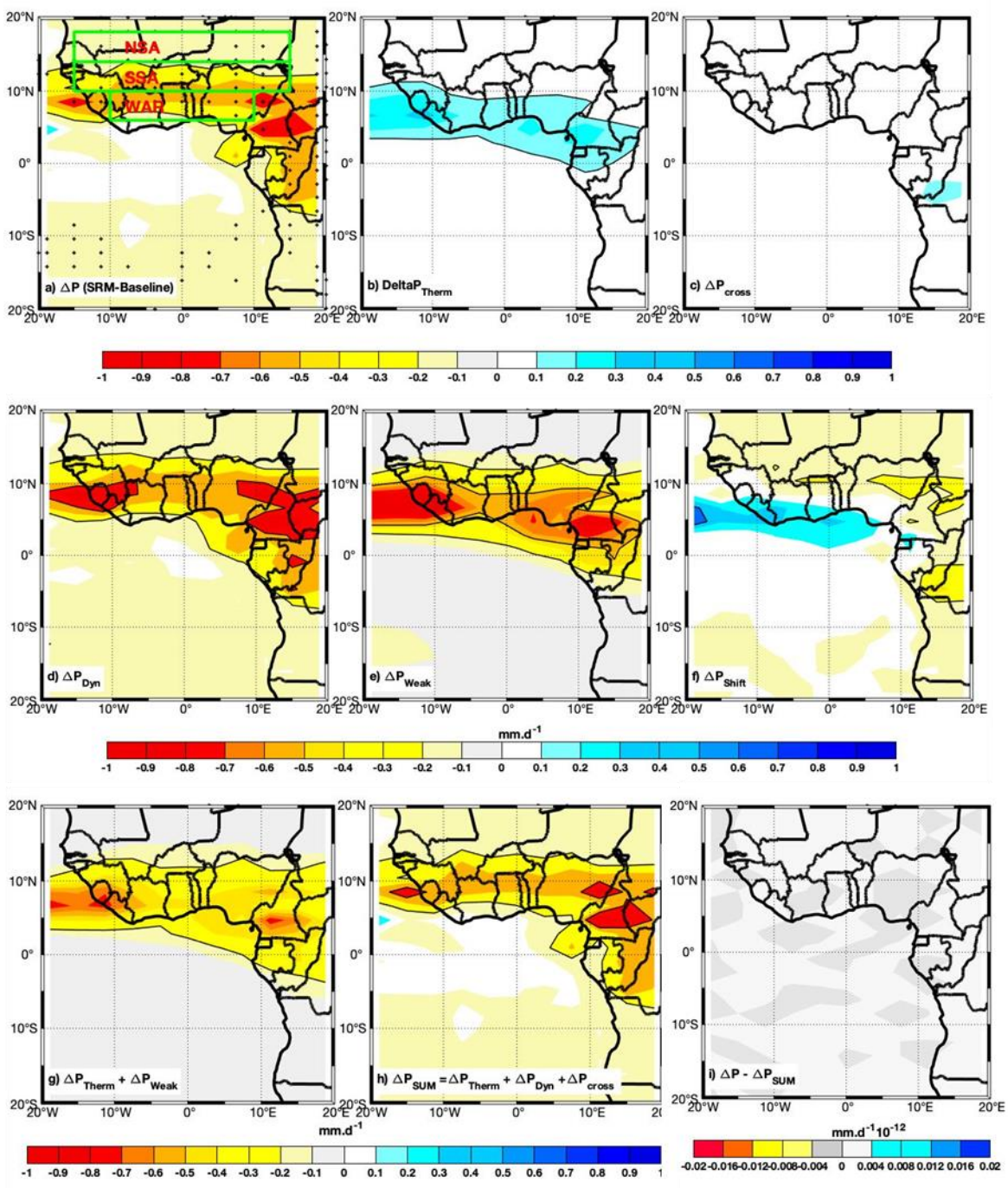


**Figure 10: (**G3 – Baseline) similar to Fig 8.

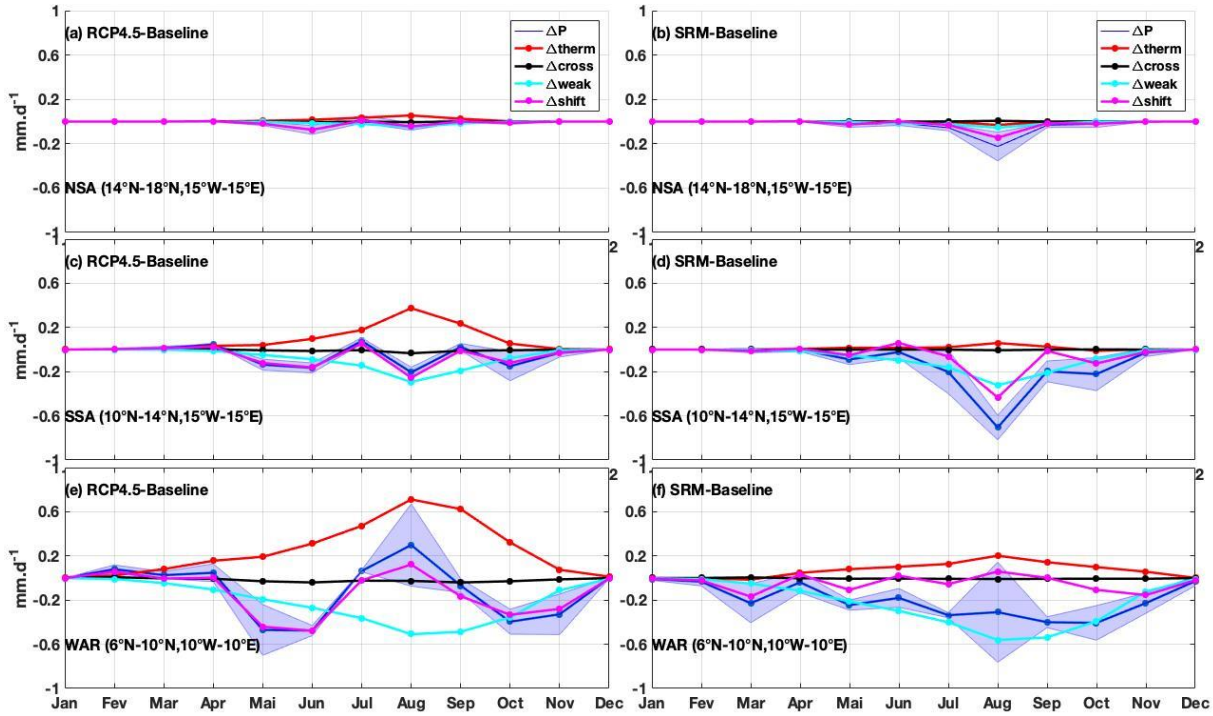


**Figure 11:** Seasonal cycles of precipitation changes and the different components of precipitation changes (see Figure 8) under RCP4.5 (left column) and G3 (IPSL-CMAP-LR) (right column) relative to the baseline for the Northern of Sahel (a and b), Southern of Sahel (c and d), and the Western Africa region (e and f). Here the nonlinear component of precipitation (ΔPcross) is added and the blue shaded areas indicating the standard error on the term of precipitation changes. Changes in precipitation are obtained as in Figures 8 and 10. All units are mm. day $^{-1}$.

The changes in P using IPSL-CMAP-LR simulations (CMIP5 and GeoMIP) with its different components decomposition for three different regions (NSA, SSA, and WAR) have been presented in West Africa (Fig. 11) similar to those defined by Da-Allada et al. (2020) who considered in their work the Northern Sahel (NSA; 18°N–14°N, 15°W–15°E), the Southern Sahel (SSA; 14°N–10°N, 15°W–15°E), and the Western Africa region (WAR; 6°N–10°N, 10°W–10°E). Under RCP4.5, slight decreases of P have been found (0.005 ± 0.075 i.e. 0.86%) and (0.03 ± 0.17 i.e. 0.8 %) in the NSA and SSA but these changes are not significant (Fig. 4.a , Fig. 10.a and 10.c) over both sub-regions contrary to those of Da-Allada et al.(2020) which found significant increase with GLENS simulations. Otherwise the increase of P (0.09±0.29 i.e. 1.04 %) has been obtained in Western Africa Region (WAR) similar trend variation in

agreement with that of Da-Allada et al. (2020). This result suggests that under RP.4.5, the increase will be moderated in WAR. Under SAG with G3 simulation, during summer period, the precipitation decreases (0.10± 0.12 i.e. 17.4%) and (0.36± 0.29 8.47 %) respectively in the NSA and SSA, this pattern is not similar to that found by Da-Allada et al.(2020) in NSA but found a slight decrease in SSA during the summer period with GLENS Simulation These results in both regions may be taken with reserve due to the non-significant change under RCP.4.5 and baseline, however Da.-Allada et al. (2020) found that deployed the SAG in these regions will be effective. The decrease by and (0.34± 0.25 i.e. 3.71%) have been noted in WAR while Da. Allada et al. (2020) obtained 0.72 ± 0.27 mm (10.87%) of decrease over this sub-region. Their decrease in P is higher than that obtained in this study, this may be due to the use of RCP8.5 simulations have accentuated effect on P. In these three regions, during the boreal summer, changes in precipitation relative to the baseline for RCP4.5 and G3 are important comparing with those of evaporation (Fig. 12) over SSA and WAR. The changes in rainfall are larger than those of evaporation in SSA and WAR regions while the change in rainfall is similar to that of evaporation in NSA region. These results are similar to those observed in Da-Allada et al. (2020) using GLENS simulation. The physical processes responsible for rainfall changes in precipitation under RCP4.5 are associated with the changes in the monsoon circulation that shifts monsoon precipitation (shift component in Fig.11). Under G3 simulation, in the three regions, changes in precipitation have the same trend as the weakened component of dynamic precipitation change (Fig.11).

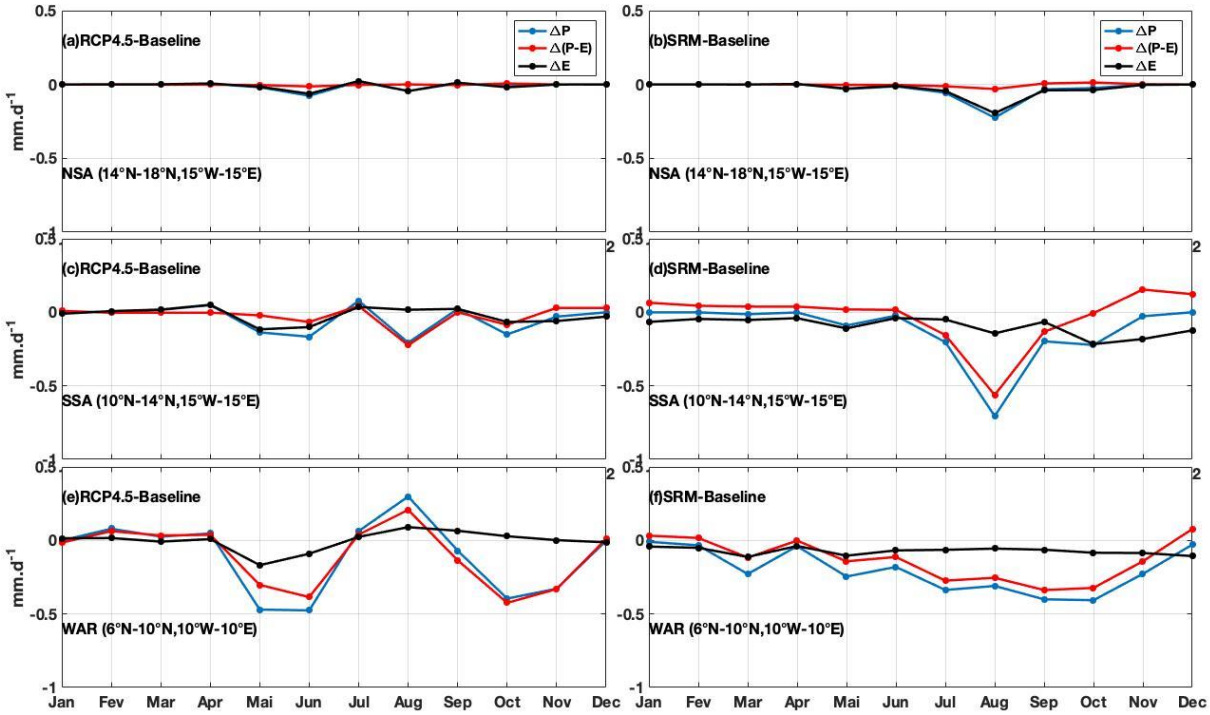


**Figure 12:** Monthly variability of precipitation, precipitation-evaporation and evaporation changes (relative to the present-day climate simulation) under RCP4.5 (left column) and G3 (right column) for the Northern of Sahel (a and b), Southern of Sahel (c and d), and the Western

Africa region (e and f). Changes are for the period 2050–2069 relative to the present-day similation. All units are mm. $Day^{-1}$

Recently, Cheng et al. (2019) computed the boreal summer efficacy of geoengineering, which balance the impacts of high GHGs emissions (ratio of Geoengineering–High-GHGs difference over that of HighGHGs–Baseline) for precipitation. The efficacy value >−1 leads to under compensation induced by geoengineering relative to baseline whereas the efficacy value <−1 suggests geoengineering leads to over compensation relative to baseline. In this work, we did not calculate the efficacy for NSA and SSA due to non-significant changes of P found under RCP4.5; therefore, we only focused our calculation in WAR. We obtained the mean efficacy value of precipitation equal to −3.51 <−1 (high over compensation) in WAR, this result is similar to that found recently by Da-Allada et al. (2020).

**Discussion**

In this study, the historical precipitation of CMIP5 models have been validated by comparing these models with CMAP and GPCP observation. The changes of precipitation under climate change and climate geo-engineering through the application of Stratospheric Aerosol Geoengineering have been determined over West Africa and Sahel region using RCP4.5 and G3/G4 models from GeoMIP simulations. These (G3/G4) GeoMIP simulations are the simulation with which SAG have been deployed. The possible impacts of SAG and the present-day scenario on precipitations within the period of (2050-2069) have been analyzed. The main mechanisms of rainfall changes have been determined using IPSL-CMA5-LR (due to availability of specific humidity data near 950hPa) basing on the methods used in Da-Allada et al. (2020).

All CMIP5 models are relatively in agreement with CMAP and GPCP precipitation. Their general patterns in estimating West African Monson precipitation mainly during July and October is comparable with observations. However, underestimation and overestimation of precipitation are also pointed out over some regions of West Africa from one model to another. CSIRO-Mk3L-1-2, BNU-ESM models present an underestimation of rainfall over the whole West Africa and Sahel Region while MPI-ESM, CNRM-CM1 models present slightly overestimation of precipitation over these regions. Statistically, the ensemble simulations of all the models shows underestimation of P in term of their behavior in estimating WAM. Recently Da-Allada et al. (2020) reported some underestimation of GLENS simulation compared with CMAP and GPCP rainfall. These model biases over certain regions of West Africa and Sahel region could be explained by the poor simulation of orographic forced ascent or the large uncertainty in the model precipitation estimates over this region (Akinsanola & Zhou, 2018; Diallo et al., 2016, Da-Allada et al.,2020).

The analysis of the precipitation changes shows relatively the decrease of precipitation over

West Africa (Table 2, & table 3) under SAG while under global warming, most of simulations shows the increase of precipitation compared with present- day simulations (Table 4). MIROC-ESM an MIROC-ESM-CHEM show increase of precipitation under G4 simulations. This is due to the biases in these models. The decrease of precipitation is observed under global warming condition (RCP4.5) with some of RCP4.5 simulations, however, the ensemble simulation and must of simulation agree with P increase under global warming (Table 4). Recently increase of precipitation has been observed under global warming (RCP8.5) and decrease of P under SAG in Da-Allada et al. (2020) using GLENS simulations. Some of opposite trend presented in this study could be explained by some higher biases in such models. Dike et al. (2014) have pointed out the overestimation of precipitation biases in some climate models over West Africa. They associated the reason to the fact that these models do not capture the changes in the Sea Surface Temperature within the Gulf of Guinea, which modulates the African monsoon circulation. These biases have revealed that the transition phase of African monsoon circulation is not well-represented by the model. However, this model simulates well the seasonal variability of precipitation in this region during summer monsoon precipitation period.

The decomposition methods (Da-Allada et al., 2020, Monerie et al. 2020, Kent et al. 2015; Chadwick et al. 2016; Rowell and Chadwick 2018) used in this work are consistent to investigate the possible causes of precipitation. This method allows understanding of the mechanisms that driven precipitation change in terms of dynamic and thermodynamic changes. Under RCP4.5, the increase of Precipitation in IPSL-CM5A-LR simulations is explained by the dynamic process. A similar result has been obtained by Da-Allada et al. (2020) to explain the changes basing on P decomposition. This method has not been applied to other models used in this work as they have lower vertical resolution and there are missing of specific humidity at near-surface pressure level in these models except IPSL-CM5A-LR model
Under SAG, we obtained previously with this model, the decrease of precipitation in West Africa and Sahel region. The dynamic terms (both weak and shift terms) are mainly responsible for the precipitation change. Recently, Da-Allada et al. (2020) emphasized that their contribution is largely associated with the low-level land-sea temperature contrast.

This work is based on precipitation changes under global warming and SAG with G3 and G4 scenarios that have been performed using CMIP5 and GeOMIP for the first time in West Africa. Recently similar work has been done using GLENS simulations in Da-Allada et al. (2020). The GLENS models show relatively the same spatial trend of shifts and changes in magnitudes of the precipitation features obtained with IPSL-CM5A-LR simulations. Monerie et al. (2020) using RCP8.5 of CMIP5 models found that the change in precipitation is explained by dynamical term of P decomposition. We found also a similar mechanism for the precipitation change under global warming, this change of P is explained by dynamic process mainly the shift component of precipitation This is similar to that obtained in Da-Allada et al. (2020) using RCP8.5 scenarios of GLENS simulations. The change of precipitation under SAG using

GeoMIP remains also the same patterns. Under GLENS, Da-Allada reported the changes in the West African Summer Monsoon precipitation which are largely explained by the reduction in land-sea thermal contrast in the lower troposphere that leads to weakened monsoon circulation and a northward shift of the monsoon precipitation patterns.

Most of CMIP5 and GeoMIP model data analysis shows that precipitation will increase over the Sahel and West African region under global warming while decrease of precipitation appears mostly under SAG. Decomposing precipitation helps to determine the mains causes of precipitation change. Basing on the decomposition methods, we fund that the change in precipitation is explained dynamical processes using IPSL-CM5A-LR model. This is consistent with Da-Allada. (2020), who found a similar behavior but using GLENS simulations, our results strengthen their finding with other climate model mainly the GeoMIP simulations. However due to biases in climate models, some of these models present opposite trend of precipitation changes (from Table 2 to table 3). This is due to the fact that some climate models such as CMIP5 and hereafter GeoMIP present significant uncertainties on their behavior representing the African Monsoon precipitation in Sahel region and also in African region (Monerie et al. (2020).

The hydrological cycle in this region can be affected by the deployment of SAG. Thus, the application of SAG in West African region using both G3 and CMIP5 simulations will over compensate the changes in precipitation in the Western Africa region. This recommends counterbalancing all warming would be going excessively far if the objective were to reestablish the Western Africa monsoon precipitation; rather, this would require restricting SAG arrangement to balancing 1/3 of RCP4.5 warming as previously proposed in Da-Allada et al. (2020) using RCP8.5 and G3 simulation of GLENS model. As the connection between global mean warming and regional precipitation change is dependent upon enormous vulnerabilities, this model outcome ought to be taken with consideration in the monitoring of future climate.

## Conclusion

This paper contributes to the analysis of monsoon precipitation on precipitation changes and the mechanisms responsible of these changes during boreal summer in West Africa using CMIP5 and GeoMIP simulations. In general, all models reproduce relatively the monsoon precipitation patterns compared with to observations data all models agree with the intensification of P during West African Monsoon period. IPSL-CMA5 –LR simulations have been used in this study to investigate the mains mechanism inducing changes of precipitation under global warming and climate geo-engineering. An increase in summer monsoon precipitation is slightly observed over West Africa Region and most accentuated over coastal zone adjacent to West Africa countries located below 10°N under RCP4.5. These changes on monsoon P under RCP4.5 are mainly driven by the dynamic process. Under G3 simulation, the decrease above 5°N during boreal summer has been reported in West Africa and Sahel region. This change of P under G3 precipitation is mainly explained by the dynamic process (both shift and weak term), which leads to a weakened monsoon circulation and a shift in the distribution of monsoon precipitation.

Three specific regions have been considered, NSA, the SSA, and the WAR similar to that of Da-Allada et al. (2020). Under RCP4.5, during the monsoon period, non-significant precipitation decreased by (0.005 ± 0.075 i.e. 0.86%) and (0.03 ± 0.17 i.e. 0.8 %) are reported at NSA and SSA respectively while rainfall increase of P (0.09±0.29 1.04 %) compared with present-day simulation in WAR region. However, with G3, relative to the baseline, the WASM rainfall, the precipitation decreases (0.10± 0.12 i.e. 17.4%) and (0.36± 0.29 i.e 8.47 %) respectively in the NSA and SSA while the decrease by and (0.34± 0.25 i.e. 3.71%) has been noted in WAR. Due to the non-significant changes over NSA and SSA, the efficacy mean has been considered only for WAR region. Using SAG will therefore have no major effect in the Sahel regions (NSA and SSA), whereas it can be over effective in the WAR. The mean efficacy ratio of SAG (−3.51) determined during the monsoon period suggests a high over compensation in WAR. In the West Africa Region, if the goal were to reestablish the Western African Monsoon precipitation, this work recommends that the organization of SAG ought to be restricted to balance 1/3 of RCP4.5, as previously suggested by Da-Allada et al. (2020)

In agreement with previous studies (e.g., Da-Allada et al, 2020, Cheng et al., 2019), our results showed that WASM precipitation decrease also under G3 simulation as they recently found with GLENS simulations. This study is a contribution to the determination of the physical processes responsible for precipitation changes in the WAR using G3. Our findings indicated that changes in precipitation in this region are largely led by the changes in the monsoon circulation which derive from the reduction of the thermal gradient induced by the application of SAG. Understanding the mechanism of the precipitation decrease will contribute to improve and implement the strategies for stratospheric aerosol injection to mitigate the effect of SAG on precipitation changes.

**Acknowledgments:**

We acknowledge the financial support of the DECIMALS fund of the Solar Radiation Management Governance Initiative, which was set up in 2010 by the Royal Society, Environmental Defense Fund and The World Academy of Sciences and is funded by the Open Philanthropy Project. All authors thank every group involved in CMIP5 model output data provided by the WHOI CMIP5 Community and we also thank the climate modeling group of the GeoMIP and the scientists managing the Earth System Grid data nodes who have assisted in making the GeoMIP output available. This work is also in the framework of the Jeune Equipe Associée à l'IRD named Variabilité de laSAlinité et Flux d'eau doUce à MultiÉchelles which is supported by Institut de Recherche pour le Développement (IRD).

**Conflicts of Interest:** The author declares no conflict of interest.

## References


Abiodun, B. J., Pal, J. S., Afiesimama, E. A., Gutowski, W. J., & Adedoyin, A. (2008). Simulation of West African monsoon using RegCM3 Part II: Impacts of deforestation and desertification. *Theoretical and Applied Climatology*, *93*(3–4), 245–261.

Akinsanola, A. A., & Zhou, W. (2018). Ensemble-based CMIP5 simulations of West African summer monsoon rainfall: Current climate andfuture changes. Theoretical and Applied Climatology, 136, 1021–1031. https://doi.org/10.1007/s00704-018-2516-3

Bala, G., Duffy, P. B., & Taylor, K. E. (2008). Impact of geoengineering schemes on the global hydrological cycle. *Proceedings of the National Academy of Sciences*, *105*(22), 7664–7669. https://doi.org/10.1073/pnas.0711648105

Bürger, G., and U. Cubasch (2015), Thedetectability of climate engineering,J. Geophys. Res. Atmos., 120,11,404–11,418, doi:10.1002/2015JD023954

Chadwick, R., Boutle, I., & Martin, G. (2013). Spatial patterns of precipitation change in CMIP5: Why the rich do not get richer in the tropics. *Journal of Climate*, *26*(11), 3803–3822.

Chadwick, R., Good, P., & Willett, K. (2016). A simple moisture advection model of specific humidity change over land in response to SST warming. *Journal of Climate*, *29*(21), 7613–7632.

Cheng, W., MacMartin, D. G., Dagon, K., Kravitz, B., Tilmes, S., Richter, J. H., Mills, M. J., & Simpson, I. R. (2019). Soil Moisture and Other Hydrological Changes in a Stratospheric Aerosol Geoengineering Large Ensemble. *Journal of Geophysical Research: Atmospheres*, *124*(23), 12773–12793. https://doi.org/10.1029/2018JD030237

Clarke, L.A.; Taylor, M.A.; Centella-Artola, A.; Williams, M.S.M.; Campbell, J.D.; Bezanilla-Morlot, A.; Stephenson, T.S. The Caribbean and 1.5 °C: Is SRM an Option? Atmosphere 2021, 12, 367. https://doi.org/10.3390/atmos12030367

Collins, W. J., Bellouin, N., Doutriaux-Boucher, M., Gedney, N., Halloran, P., Hinton, T., Hughes, J., Jones, C. D., Joshi, M., & Liddicoat, S. (2011). Development and evaluation of an Earth-System model–HadGEM2. *Geosci. Model Dev. Discuss*, *4*(2), 997–1062.

Crutzen, P. J. (2006). Albedo Enhancement by Stratospheric Sulfur Injections: A Contribution to Resolve a Policy Dilemma? *Climatic Change*, *77*(3), 211. https://doi.org/10.1007/s10584-006-9101-y

Da-Allada, C. Y., Baloïtcha, E., Alamou, E. A., Awo, F. M., Bonou, F., Pomalegni, Y., Biao, E. I., Obada, E., Zandagba, J. E., Tilmes, S., & Irvine, P. J. (2020). Changes in West African Summer Monsoon Precipitation Under Stratospheric Aerosol Geoengineering. *Earth's Future*, *8*(7), e2020EF001595. https://doi.org/10.1029/2020EF001595

Dagon, K., & Schrag, D. P. (2016). Exploring the Effects of Solar Radiation Management on Water Cycling in a Coupled Land–Atmosphere Model. *Journal of Climate*, *29*(7), 2635–2650. https://doi.org/10.1175/JCLI-D-15-0472.1

739 Dagon, K., & Schrag, D. P. (2017). Regional Climate Variability Under Model Simulations of
740 Solar Geoengineering. *Journal of Geophysical Research: Atmospheres*, *122*(22),
741 12,106-12,121. https://doi.org/10.1002/2017JD027110
742 Diallo, I., Giorgi, F., Tall, M., Mariotti, L., & Gaye, A. T. (2016). Projected changes of
743 summer monsoon extreme and hydroclimatic regimesover West Africa for the twenty-
744 first century. Climate Dynamics, 47, 3931–3954. https://doi.org/10.1007/s00382-016-
745 3,052-4
746 Dike, Victor, Marilia Shimizu, Mohamadou Diallo, Zhaohui Lin, Okey Nwofor, and Theo
747 Chineke. "Modelling Present and Future African Climate Using CMIP5 Scenarios in
748 HadGEM2-ES." International Journal of Climatology 35 (June 1, 2015).
749 https://doi.org/10.1002/joc.4084.
750 Dong, B., & Sutton, R. (2015). Dominant role of greenhouse-gas forcing in the recovery of
751 Sahel rainfall. *Nature Climate Change*, *5*(8), 757–760.
752 https://doi.org/10.1038/nclimate2664
753 Dufresne, J.-L., Foujols, M.-A., Denvil, S., Caubel, A., Marti, O., Aumont, O., Balkanski, Y.,
754 Bekki, S., Bellenger, H., Benshila, R., Bony, S., Bopp, L., Braconnot, P., Brockmann,
755 P., Cadule, P., Cheruy, F., Codron, F., Cozic, A., Cugnet, D., … Vuichard, N. (2013).
756 Climate change projections using the IPSL-CM5 Earth System Model: From CMIP3 to
757 CMIP5. *Climate Dynamics*, *40*(9), 2123–2165. https://doi.org/10.1007/s00382-012-
758 1636-1
759 Froidurot, S., & Diedhiou, A. (2017). Characteristics of wet and dry spells in the West African
760 monsoon system. *Atmospheric Science Letters*, *18*(3), 125–131.
761 Gaetani, M., Flamant, C., Bastin, S., Janicot, S., Lavaysse, C., Hourdin, F., Braconnot, P., &
762 Bony, S. (2017). West African monsoon dynamics and precipitation: The competition
763 between global SST warming and CO2 increase in CMIP5 idealized simulations.
764 *Climate Dynamics*, *48*(3–4), 1353–1373. https://doi.org/10.1007/s00382-016-3146-z
765 Gleckler, P. J., Taylor, K. E., & Doutriaux, C. (2008). Performance metrics for climate
766 models. *Journal of Geophysical Research: Atmospheres*, *113*(D6).
767 https://doi.org/10.1029/2007JD008972
768 Gong, C., & Eltahir, E. (1996). Sources of moisture for rainfall in West Africa. *Water*
769 *Resources Research*, *32*(10), 3115–3121.
770 Govindasamy, B., & Caldeira, K. (2000). Geoengineering Earth's radiation balance to mitigate
771 CO2-induced climate change. *Geophysical Research Letters*, *27*(14), 2141–2144.
772 Haywood, J. M., Jones, A., Bellouin, N., & Stephenson, D. (2013). Asymmetric forcing from
773 stratospheric aerosols impacts Sahelian rainfall. *Nature Climate Change*, *3*(7), 660–
774 665. https://doi.org/10.1038/nclimate1857
775 Heckendorn, P., Weisenstein, D., Fueglistaler, S., Luo, B. P., Rozanov, E., Schraner, M.,
776 Thomason, L. W., & Peter, T. (2009). The impact of geoengineering aerosols on
777 stratospheric temperature and ozone. *Environmental Research Letters*, *4*(4), 045108.
778 https://doi.org/10.1088/1748-9326/4/4/045108

779 Held, I. M., & Soden, B. J. (2006). Robust responses of the hydrological cycle to global
780 warming. *Journal of Climate*, *19*(21), 5686–5699.
781 Hourdin, F., Foujols, M.-A., Codron, F., Guemas, V., Dufresne, J.-L., Bony, S., Denvil, S.,
782 Guez, L., Lott, F., Ghattas, J., Braconnot, P., Marti, O., Meurdesoif, Y., & Bopp, L.
783 (2013). Impact of the LMDZ atmospheric grid configuration on the climate and
784 sensitivity of the IPSL-CM5A coupled model. *Climate Dynamics*, *40*(9–10), 2167–
785 2192. https://doi.org/10.1007/s00382-012-1411-3
786 Huffman, G. J., Adler, R. F., Arkin, P., Chang, A., Ferraro, R., Gruber, A., Janowiak, J.,
787 McNab, A., Rudolf, B., & Schneider, U. (1997). The Global Precipitation Climatology
788 Project (GPCP) Combined Precipitation Dataset. *Bulletin of the American*
789 *Meteorological Society*, *78*(1), 5–20. https://doi.org/10.1175/1520-
790 0477(1997)078<0005:TGPCPG>2.0.CO2
791 Janicot, S. (1992). Spatiotemporal variability of West African rainfall. Part I: Regionalizations
792 and typings. *Journal of Climate*, *5*(5), 489–497.
793 Jones, A. C., Hawcroft, M. K., Haywood, J. M., Jones, A., Guo, X., & Moore, J. C. (2018).
794 Regional Climate Impacts of Stabilizing Global Warming at 1.5 K Using Solar
795 Geoengineering. *Earth's Future*, *6*(2), 230–251.
796 https://doi.org/10.1002/2017EF000720
797 Jones, A., Haywood, J., Boucher, O., Kravitz, B., & Robock, A. (2010). Geoengineering by
798 stratospheric $SO_2$ injection: Results from the Met Office HadGEM2 climate model and
799 comparison with the Goddard Institute for Space Studies ModelE. *Atmospheric*
800 *Chemistry and Physics*, *10*(13), 5999–6006. https://doi.org/10.5194/acp-10-5999-2010
801 Kent, C., Chadwick, R., & Rowell, D. P. (2015). Understanding uncertainties in future
802 projections of seasonal tropical precipitation. *Journal of Climate*, *28*(11), 4390–4413.
803 Kim, K. H., Lim, T., Park, K. J., Koo, H.-C., Kim, M. J., & Kim, J. J. (2015). Investigation of
804 Cu growth phenomena on Ru substrate during electroless deposition using hydrazine
805 as a reducing agent. *Electrochimica Acta*, *151*, 249–255.
806 https://doi.org/10.1016/j.electacta.2014.11.036
807 Kravitz, B., Caldeira, K., Boucher, O., Robock, A., Rasch, P. J., Alterskj\a er, K., Karam, D.
808 B., Cole, J. N., Curry, C. L., & Haywood, J. M. (2013). Climate model response from
809 the geoengineering model intercomparison project (GeoMIP). *Journal of Geophysical*
810 *Research: Atmospheres*, *118*(15), 8320–8332.
811 Kravitz, B., MacMartin, D. G., Mills, M. J., Richter, J. H., Tilmes, S., Lamarque, J.-F.,
812 Tribbia, J. J., & Vitt, F. (2017). First Simulations of Designing Stratospheric Sulfate
813 Aerosol Geoengineering to Meet Multiple Simultaneous Climate Objectives. *Journal*
814 *of Geophysical Research: Atmospheres*, *122*(23), 12,616-12,634.
815 https://doi.org/10.1002/2017JD026874
816 Kravitz, B., MacMartin, D. G., Tilmes, S., Richter, J. H., Mills, M. J., Cheng, W., Dagon, K.,
817 Glanville, A. S., Lamarque, J.-F., Simpson, I. R., Tribbia, J., & Vitt, F. (2019).
818 Comparing Surface and Stratospheric Impacts of Geoengineering With Different SO2

819 Injection Strategies. *Journal of Geophysical Research: Atmospheres*, *124*(14), 7900–
820 7918. https://doi.org/10.1029/2019JD030329
821 Kravitz, B., Robock, A., Boucher, O., Schmidt, H., Taylor, K. E., Stenchikov, G., & Schulz,
822 M. (2011). The geoengineering model intercomparison project (GeoMIP). *Atmospheric*
823 *Science Letters*, *12*(2), 162–167.
824 Lamb, P. J. (1982). *Persistence of Subsaharan drought | Nature*.
825 https://www.nature.com/articles/299046a0
826 Launder, Brian, & Thompson, J. Michael T. (2010). Geo-Engineering Climate Change:
827 Environmental Necessity or Pandora's Box? *Civil Engineering—ASCE, 2010, Vol. 80,*
828 *Issue 5, Pg. 84-85*, *80*(5), 84–85.
829 Lazenby, M. J., Todd, M. C., Chadwick, R., & Wang, Y. (2018). Future Precipitation
830 Projections over Central and Southern Africa and the Adjacent Indian Ocean: What
831 Causes the Changes and the Uncertainty? *Journal of Climate*, *31*(12), 4807–4826.
832 https://doi.org/10.1175/JCLI-D-17-0311.1
833 Le Barbé, L., Lebel, T., & Tapsoba, D. (2002). Rainfall variability in West Africa during the
834 years 1950–90. *Journal of Climate*, *15*(2), 187–202.
835 Lélé, M. I., Leslie, L. M., & Lamb, P. J. (2015). Analysis of low-level atmospheric moisture
836 transport associated with the West African Monsoon. *Journal of Climate*, *28*(11),
837 4414–4430.
838 Lenton, T. M., & Vaughan, N. E. (2009). Interactive comment on "The radiative forcing
839 potential of different climate geoengineering options" by T. M. Lenton and N. E.
840 Vaughan. *Discussion Paper*, 15.
841 Loikith, P. C., Waliser, D. E., Lee, H., Kim, J., Neelin, J. D., Lintner, B. R., McGinnis, S.,
842 Mattmann, C. A., & Mearns, L. O. (2015). Surface Temperature Probability
843 Distributions in the NARCCAP Hindcast Experiment: Evaluation Methodology,
844 Metrics, and Results. *Journal of Climate*, *28*(3), 978–997.
845 https://doi.org/10.1175/JCLI-D-13-00457.1
846 MacMartin, D. G., Wang, W., Kravitz, B., Tilmes, S., Richter, J. H., & Mills, M. J. (2019).
847 Timescale for Detecting the Climate Response to Stratospheric Aerosol
848 Geoengineering. *Journal of Geophysical Research: Atmospheres*, *124*(3), 1233–1247.
849 https://doi.org/10.1029/2018JD028906
850 Madec, G. (2016). *NEMO ocean engine*. *3.6*, 396.
851 Mera, R., Laing, A. G., & Semazzi, F. (2014). Moisture variability and multiscale interactions
852 during spring in West Africa. *Monthly Weather Review*, *142*(9), 3178–3198.
853 Mignot, J., Swingedouw, D., Deshayes, J., Marti, O., Talandier, C., Séférian, R., Lengaigne,
854 M., & Madec, G. (2013). On the evolution of the oceanic component of the IPSL
855 climate models from CMIP3 to CMIP5: A mean state comparison. *Ocean Modelling*,
856 *72*, 167–184. https://doi.org/10.1016/j.ocemod.2013.09.001

Monerie, PA., Wainwright, C.M., Sidibe, M. et al. Model uncertainties in climate change impacts on Sahel precipitation in ensembles of CMIP5 and CMIP6 simulations. Clim Dyn 55, 1385–1401 (2020). https://doi.org/10.1007/s00382-020-05332-0

Monerie, P., Robson, J., Dong, B., Hodson, D. L. R., & Klingaman, N. P. (2019). Effect of the Atlantic Multidecadal Variability on the Global Monsoon. *Geophysical Research Letters*, *46*(3), 1765–1775. https://doi.org/10.1029/2018GL080903

Nicholson, S. E. (2013). The West African Sahel: A Review of Recent Studies on the Rainfall Regime and Its Interannual Variability. *ISRN Meteorology*, *2013*, 1–32. https://doi.org/10.1155/2013/453521

Nicholson, S. E., & Grist, J. P. (2003). The seasonal evolution of the atmospheric circulation over West Africa and equatorial Africa. *Journal of Climate*, *16*(7), 1013–1030.

Niemeier, U., Schmidt, H., Alterskjær, K., & Kristjánsson, J. E. (2013). Solar irradiance reduction via climate engineering: Impact of different techniques on the energy balance and the hydrological cycle. *Journal of Geophysical Research: Atmospheres*, *118*(21), 11–905.

Odoulami, Romaric C., Mark New, Piotr Wolski, Gregory Guillemet, Izidine Pinto, Christopher Lennard, Helene Muri, and Simone Tilmes. "Stratospheric Aerosol Geoengineering Could Lower Future Risk of `Day Zero' Level Droughts in Cape Town." Environmental Research Letters 15, no. 12 (November 2020): 124007. https://doi.org/10.1088/1748-9326/abbf13.

Okoro, U. K., Chen, W., & Nath, D. (2018). Recent variations in geopotential height associated with West African monsoon variability. *Meteorology and Atmospheric Physics*, *131*(3), 553–565. https://doi.org/10.1007/s00703-018-0593-6

Parth Sarthi, P., Kumar, P., & Ghosh, S. (2016). Possible future rainfall over Gangetic Plains (GP), India, in multi-model simulations of CMIP3 and CMIP5. *Theoretical and Applied Climatology*, *124*(3), 691–701. https://doi.org/10.1007/s00704-015-1447-5

Pinto, I., Jack, C., Lennard, C., Tilmes, S., & Odoulami, R. C. (2020). Africa's Climate Response to Solar Radiation Management With Stratospheric Aerosol. *Geophysical Research Letters*, *47*(2), e2019GL086047. https://doi.org/10.1029/2019GL086047

Pomposi, C., Kushnir, Y., & Giannini, A. (2015). Moisture budget analysis of SST-driven decadal Sahel precipitation variability in the twentieth century. *Climate Dynamics*, *44*(11), 3303–3321. https://doi.org/10.1007/s00382-014-2382-3

Redelsperger, J. L., Mahé, F., & Carlotti, P. (2001). A Simple And General Subgrid Model Suitable Both For Surface Layer And Free-Stream Turbulence. *Boundary-Layer Meteorology*, *101*(3), 375–408. https://doi.org/10.1023/A:1019206001292

Redelsperger, J.-L., Thorncroft, C. D., Diedhiou, A., Lebel, T., Parker, D. J., & Polcher, J. (2006). African Monsoon Multidisciplinary Analysis: An International Research Project and Field Campaign. *Bulletin of the American Meteorological Society*, *87*(12), 1739–1746. https://doi.org/10.1175/BAMS-87-12-1739

Robock, A., Marquardt, A., Kravitz, B., & Stenchikov, G. (2009). Benefits, risks, and costs of stratospheric geoengineering. *Geophysical Research Letters*, *36*(19). https://doi.org/10.1029/2009GL039209

Robock, A., Oman, L., & Stenchikov, G. L. (2008). Regional climate responses to geoengineering with tropical and Arctic $SO_2$ injections. *Journal of Geophysical Research: Atmospheres*, *113*(D16).

Roehrig, R., Bouniol, D., Guichard, F., Hourdin, F., & Redelsperger, J.-L. (2013). The Present and Future of the West African Monsoon: A Process-Oriented Assessment of CMIP5 Simulations along the AMMA Transect. *Journal of Climate*, *26*(17), 6471–6505. https://doi.org/10.1175/JCLI-D-12-00505.1

Sanogo, S., Fink, A. H., Omotosho, J. A., Ba, A., Redl, R., & Ermert, V. (2015). Spatio-temporal characteristics of the recent rainfall recovery in West Africa. *International Journal of Climatology*, *35*(15), 4589–4605.

Sheffield, J., Barrett, A. P., Colle, B., Nelun Fernando, D., Fu, R., Geil, K. L., Hu, Q., Kinter, J., Kumar, S., Langenbrunner, B., Lombardo, K., Long, L. N., Maloney, E., Mariotti, A., Meyerson, J. E., Mo, K. C., David Neelin, J., Nigam, S., Pan, Z., … Yin, L. (2013). North American Climate in CMIP5 Experiments. Part I: Evaluation of Historical Simulations of Continental and Regional Climatology. *Journal of Climate*, *26*(23), 9209–9245. https://doi.org/10.1175/JCLI-D-12-00592.1

Tilmes, S., Fasullo, J., Lamarque, J.-F., Marsh, D. R., Mills, M., Alterskj\a er, K., Muri, H., Kristjánsson, J. E., Boucher, O., & Schulz, M. (2013). The hydrological impact of geoengineering in the Geoengineering Model Intercomparison Project (GeoMIP). *Journal of Geophysical Research: Atmospheres*, *118*(19), 11–036.

Tilmes, S., Fasullo, J., Lamarque, J.-F., Marsh, D. R., Mills, M., Alterskjær, K., Muri, H., Kristjánsson, J. E., Boucher, O., Schulz, M., Cole, J. N. S., Curry, C. L., Jones, A., Haywood, J., Irvine, P. J., Ji, D., Moore, J. C., Karam, D. B., Kravitz, B., … Watanabe, S. (2013). The hydrological impact of geoengineering in the Geoengineering Model Intercomparison Project (GeoMIP). *Journal of Geophysical Research: Atmospheres*, *118*(19), 11,036-11,058. https://doi.org/10.1002/jgrd.50868

Tilmes, S., Garcia, R. R., Kinnison, D. E., Gettelman, A., & Rasch, P. J. (2009). Impact of geoengineered aerosols on the troposphere and stratosphere. *Journal of Geophysical Research: Atmospheres*, *114*(D12). https://doi.org/10.1029/2008JD011420

Tilmes, S., Richter, J. H., Kravitz, B., MacMartin, D. G., Mills, M. J., Simpson, I. R., Glanville, A. S., Fasullo, J. T., Phillips, A. S., Lamarque, J.-F., Tribbia, J., Edwards, J., Mickelson, S., & Gosh, S. (2018). CESM1(WACCM) Stratospheric Aerosol Geoengineering Large Ensemble (GLENS) Project. *Bulletin of the American Meteorological Society*. https://doi.org/10.1175/BAMS-D-17-0267.1

Tjiputra, J. F., Grini, A., & Lee, H. (2016). Impact of idealized future stratospheric aerosol injection on the large-scale ocean and land carbon cycles. *Journal of Geophysical Research: Biogeosciences*, *121*(1), 2–27. https://doi.org/10.1002/2015JG003045

Watanabe, S., Hajima, T., Sudo, K., Nagashima, T., Takemura, T., Okajima, H., Nozawa, T., Kawase, H., Abe, M., & Yokohata, T. (2011). MIROC-ESM 2010: Model description and basic results of CMIP5-20c3m experiments. *Geoscientific Model Development*, *4*(4), 845.

Weller, E., Jakob, C., & Reeder, M. J. (2019). Understanding the Dynamic Contribution to Future Changes in Tropical Precipitation From Low-Level Convergence Lines. *Geophysical Research Letters*, *46*(4), 2196–2203. https://doi.org/10.1029/2018GL080813

Xie, P., & Arkin, P. A. (1997). Global precipitation: A 17-year monthly analysis based on gauge observations, satellite estimates, and numerical model outputs. *Bulletin of the American Meteorological Society*, *78*(11), 2539–2558.

Xie, S.-P. (1999). A Dynamic Ocean–Atmosphere Model of the Tropical Atlantic Decadal Variability. *Journal of Climate*, *12*(1), 64–70. https://doi.org/10.1175/1520-0442(1999)012<0064:ADOAMO>2.0.CO;2

Xu, Y., Lin, L., Tilmes, S., Dagon, K., Xia, L., Diao, C., Cheng, W., Wang, Z., Simpson, I., & Burnell, L. (2020). Climate engineering to mitigate the projected 21st-century terrestrial drying of the Americas: A direct comparison of carbon capture and sulfur injection. *Earth System Dynamics*, *11*(3), 673–695. https://doi.org/10.5194/esd-11-673-2020

Xue, Y., & Shukla, J. (1993). The influence of land surface properties on Sahel climate. Part 1: Desertification. *Journal of Climate*, *6*(12), 2232–2245.